Available online at www.sciencedirect.com

ScienceDirect

Soils and Foundations 66 (2026) 101879

www.elsevier.com/locate/sandf

Technical Paper

A comparative understanding of variable SPT energy measurement in practice

M.E. Yadhunandan [a], P. Anbazhagan [a,*]

[a] Department of Civil Engineering, Indian Institute of Science, Bangalore 560012, India

Received 19 September 2025; received in revised form 7 September 2026; accepted 14 September 2026

Abstract

Accurate measurements of hammer energy are essential for reliable interpretation of the Standard Penetration Test (SPT). While energy variability is well-documented, standards often recommend measurements at a few depths or assume rig efficiencies. In many countries, these measurements are rarely performed, and there is a lack of guidance on sensor specifications and measurement frequency. This study addresses these gaps through a two-phase investigation. First, a custom 2-channel system (using either a 5000g/10000g accelerometer) that measures Energy Transfer Ratio (ETR) simultaneously at both the anvil and sampler levels, was compared with a commercial 4-channel system (10000g accelerometers) that can only measure ETR at the anvil level. The extensive laboratory and field comparison confirmed the reliability of the simpler 2-channel system, with ETR differences typically within ±5%. The second phase involved a large-scale field study with the 2-channel system across 77 boreholes (314 SPTs) at five test sites. This revealed substantial ETR variability across different rigs, even under uniform soil conditions. Anvil and sampler ETRs ranged from 29% to 78% and 21% to 54%, respectively, highlighting significant energy loss along the drill rods. These findings highlight the value of depth-wise ETR measurements for improving SPT energy correction and support future refinement of current SPT practice/standards.

Keywords: Standard Penetration Test (SPT); Energy Transfer Ratio (ETR); Hammer energy measurement; Instrumented rod; Sampler-level energy measurement; Field validation; Rig variability

AbbreviationsSPT, Standard Penetration Test; ETR, Energy Transfer Ratio; 2C-5000g, 2-channel instrumented rod with 5000g accelerometer; 2C-10000g, 2-channel instrumented rod with 10,000g accelerometer; 4C-10000g, 4-channel instrumented rod with 10,000g accelerometers; DAQ, Data Acquisition System; UCS, Unconfined Compressive Strength; AW, NW, BW, Types of drill rods (based on dimensions and threading standards); RMH, Rotary drill rig with rope and pulley for Manual lifting Hammer; RSH, Rotary drill rig with Spool winch for lifting Hammer; HSH, Hydraulic drill rig with Spool winch for lifting Hammer; HTH, Hydraulic drill rig with auto Trip Hammer; MAH, Multipurpose drill rig with Automatic Hammer; SD, Standard Deviation; g, Acceleration due to gravity (used in accelerometer e.g., 5000g); E, Energy transferred during impact (Joules); $F(t)$, Time-dependent axial force (Newtons); $V(t)$, Time-dependent axial velocity (meters per second); t, Time (seconds); FV, Force-Velocity Method; FVCD, Force or Velocity Change Direction method; R^2, Coefficient of Determination; MAE, Mean Absolute Error; Ns, Not specified; PDA, Pile Driving Analyzer; PDM, Pile Driving Monitor; GRLWEAP, A software used in some studies for wave equation analysis.; HSC, High-Speed Camera; iBPT, Instrumented Becker Penetration Test

* Corresponding author.
E-mail address: anbazhagan@iisc.ac.in (P. Anbazhagan).

https://doi.org/10.1016/j.sandf.2026.101879
0038-0806/

1. Introduction

The Standard Penetration Test (SPT) is the most widely used geotechnical site investigation, valued globally for its simplicity, cost-effectiveness, and extensive empirical correlations with soil properties. The test measures the number of hammer blows (N-value) required to drive a split-spoon sampler to a specific depth (the final 30 cm of a total 45 cm penetration, following an initial 15 cm seating drive). Due to significant global variations in SPT equipment and procedures, the concept of energy correction was introduced, whereby all N-values are normalized to a standard 60% energy efficiency (N_{60}). This is a critical step now incorporated into major international standards, including for liquefaction potential assessment (“ASTM D6066-11,” 2011; “IS 1893 (Part 1),” 2016). The reliability of N-values for geotechnical design (including the estimations of bearing capacity, liquefaction potential, and settlement) is highly dependent on the actual energy transferred to the drill rod during each hammer blow (Anbazhagan et al., 2022a; Bolton Seed et al., 1985; Cubrinovski and Ishihara, 1999; Skempton, 1986). Among the various corrections applied to the measured N-value (such as borehole diameter, sampler liner, rod length, and dilatancy corrections), overburden and energy corrections are the most predominant and widely adopted (Anbazhagan et al., 2022b).

Despite the acceptance of energy correction, international standards provide inconsistent and often insufficient guidance. While standards like ASTM (“ASTM D1586-18,” 2018; “ASTM D4633-16,” 2016; “ASTM D6066-11,” 2011) outline the fundamental procedure and provide guidance for energy measurement, the latter recommends ETR measurement at only three test depths per test site. Eurocode 7 promotes equipment standardization and mandates quality control during field testing, but allows energy correction factors to be defined by national annexes (“BS EN ISO 22476-3:2005+A1:2011,” 2005). Countries like Japan and New Zealand, where seismic risk is high, enforce strict controls on energy normalization, particularly for liquefaction hazard assessments (“JIS 1219,” 2013; Youd and Idriss, 2001). However, even in developed countries, energy measurement is usually limited to a few depths or relies on calibration-based correction factors, rather than full-depth, blow-wise measurements (“AS 1289.6.3.1.,” 2004; “ASTM D4633-16,” 2016; “GB 50021-2001,” 2001; Matsumoto et al., 2015). As summarised in Table A1 (Appendix A1), published studies demonstrate a wide variation in hammer types adopted globally, each operates at different levels of mechanical efficiency and impact consistency. The ETR values reported across these countries vary widely, ranging from as low as 25% to values as high as 80% (Aoki et al., 2007; Tsai et al., 2004).

Furthermore, SPT energy measurement systems typically use strain gauges or load cells together with accelerometers mounted on instrumented rods. As shown in Table A1 (Appendix A1), previous studies have used accelerometers with different capacities, most commonly 5000g and 10000g (Daniel and Howie, 2005; Howie et al., 2003; Lukiantchuki et al., 2017). The choice of sensor capacity depends on expected impact intensity and field conditions. While higher-capacity accelerometers (e.g., 10,000g) reduce the risk of signal saturation during strong impacts, they are generally more expensive. If lower-capacity sensors (e.g., 5000g) can reliably capture the impact response, they may offer a more economical option for routine testing. This is particularly important because SPT is a repetitive impact test; sensor durability, especially at the sampler level within boreholes containing water and drilling fluids, must also be considered. Furthermore, ASTM (“ASTM D4633-16,” 2016) highlights that multi-channel instrumentation be used to reduce potential errors caused by bending, misalignment, or signal irregularities in drill rods. As a result, current commercial systems use four-channel configurations. However, multi-channel systems increase instrumentation complexity, cost, and cable management requirements. These challenges become more significant when attempting sampler-level measurements within a standard borehole, where multiple cables must pass alongside SPT rod. From a theoretical perspective, the Force-Velocity (FV) method requires only one force and one acceleration measurement to compute transferred energy. Therefore, a simplified 2-channel configuration may provide a practical and economical alternative, provided that its accuracy is carefully validated against established multi-channel systems.

Additionally, the accuracy of site investigations is strongly influenced by the number of investigation points, yet no quantitative guidelines are available for selecting the appropriate number of SPTs to achieve a desired level of accuracy (Guan and Wang, 2020; Juang et al., 2009; Muduli and Das, 2015). This limited sampling assumes uniform energy delivery, an assumption often invalidated by field conditions involving multiple rigs, varied hammer types, and operator inconsistencies (Anbazhagan et al., 2022b; Clayton, 1995). Similarly, the requirement for normalized N-value determination for liquefaction assessment is addressed inconsistently, with only a few regions offering structured protocols. This highlights a critical gap: the assumption of a constant average ETR (e.g., 60%) is not universally valid, and this practice can lead to significant errors in geotechnical design outcomes. Although numerous studies have reported ETR values under various field configurations (Table A1, Appendix A1), most investigations have relied on limited-depth measurements or averaged efficiency values for a given rig or hammer type. Detailed blow-wise energy monitoring across multiple rigs and depths remains relatively limited in the literature. Therefore, despite extensive documentation of ETR ranges worldwide, there remains a need for a systematic evaluation of rig and hammer variability using consistent instrumentation and depth-wise measurements.

Inaccurate estimation of ETR directly affects the corrected N_{60} values and consequently all design and engineering interpretations derived from them (Anbazhagan et al., 2021). Overestimation of ETR may lead to a low corrected N-value, resulting in an unsafe bearing-capacity assessment and an unconservative liquefaction evaluation. Conversely, underestimating ETR can lead to overly conservative designs, thereby increasing foundation costs. Since SPT-based correlations are widely used to estimate bearing capacity, stiffness, settlement, and liquefaction resistance, even moderate errors in the assumed energy efficiency can propagate into significant design discrepancies. Therefore, reliable, depth-wise SPT energy measurement can improve the accuracy of corrected N-values and contribute to safer and more economical geotechnical engineering practice (Anbazhagan et al., 2022b).

The problem is compounded by two common and flawed assumptions in practice. First, practitioners often rely on a single assumed equipment efficiency (ETR) for a given hammer type, such as approximately 80% efficiency for an automatic hammer (Honeycutt et al., 2014). However, the actual performance of these systems varies significantly with maintenance, environmental conditions, component wear, and operator handling (Bolton Seed et al., 1985; Briaud and Gibbens, 1999). Second, even when measurements are performed, there is a widespread assumption that a few spot measurements can represent the average ETR for an entire borehole or project site. This overlooks the substantial variability in energy delivery across rigs and SPT depths, even under identical soil conditions. This issue is particularly pronounced in developing countries, where projects often use non-standard components from different contractors simultaneously (Anbazhagan et al., 2022b). The reliance on these inaccurate assumptions, rather than direct, depth-wise measurements, compromises the accuracy of corrected N-values and can lead to significant errors in estimating soil properties and liquefaction potential.

The present study builds on the authors' earlier work on SPT energy measurement. The 2-channel SPT-HEMA system, laboratory setup, FVCD method, and energy measurements at the anvil and sampler levels were developed and evaluated in previous studies (Anbazhagan et al., 2021, 2022a, 2022b; Yadhunandan and Anbazhagan, 2025, 2026) and are used here as established tools for the proposed work. To address research gaps, this study was carried out in two phases. Phase I was designed to comparatively evaluate the measurement system used in this study. A custom 2-channel instrumented rod system was tested with two accelerometer capacities (5000g and 10,000g), and its performance was compared with a commercial 4-channel system (10,000g) to assess differences in signal capture and energy estimation. The purpose of this phase was to (i) verify the sufficiency of the 2-channel configuration, (ii) evaluate whether lower-capacity accelerometers (5000g) are sufficient for SPT impact measurement, and (iii) ensure that the 2-channel system produces results comparable to established instrumentation before the large-scale deployment. Phase II focused on investigating ETR variability under real project conditions. The 2-channel system was deployed at multiple project sites with uniform soils, but with rigs equipped with varied hammer mechanisms, release systems, and SPT components to assess the effects of the number of ETR measurements within a borehole and across sites. The novelty of the present study lies in the direct comparison of 2-channel and 4-channel systems with different accelerometer capacities and in the systematic evaluation of ETR variability using an extensive field dataset and the number of energy measurements required to represent SPT energy behaviour in practice. The results show that limited-depth averages do not represent actual energy transfer, as ETR varied substantially across rigs and depths. These findings highlight the importance of recording energy at representative depths or, where practical, at every SPT depth, together with blow-wise measurements. The results may also assist future improvements in SPT practice and standards. By separating system validation (Phase I) from field variability assessment (Phase II), the study ensures both measurement reliability and the practical applicability of the findings.

2. Methodology and experiments

2.1. Energy measurement and energy transfer ratio

Accurate hammer energy measurement in the SPT requires recording the time history of force and acceleration (or derived velocity) during each hammer impact. In practice, instrumented rods with strain gauges and accelerometers mounted near the anvil level are widely used (Briaud and Gibbens, 1999; Schmertmann and Palacios, 1979). The standard approach for estimating ETR is the FV method, which integrates force and velocity over a fixed "tension cutoff" duration, typically represented as a 2 L/c window (where L is the drill rod length in m, and c is the stress-wave speed in the drill rod in m/s). These signals enable computation of the energy using Eq. (1).

$$ETR(\%) = \frac{E_{FV}}{PE} * 100 = \frac{\int_{t=0}^{t=2L/c} F(t) * V(t)dt}{PE} * 100 \quad (1)$$

where: ETR = Energy Transfer Ratio (in %), E_{FV} = energy measured using the FV method (in Joules), PE = Potential energy of the hammer impact (in Joules), t = stress wave travel time (in sec), L = drill rod length from the measurement point (generally just below the anvil) to the bottom end of the sampler (in m), c = stress wave speed in the drill rod (in m/s), F(t) = measured force (in N), V(t) = particle velocity obtained by integrating the measured acceleration (in m/s).

The fixed 2L/c window of the FV method has limitations, particularly for short rods where reflected waves may arrive before full energy transfer. Reflections are also difficult to identify in typical force-acceleration records. To overcome these limitations, the Force or Velocity Change Direction (FVCD) method was recently developed and experimentally validated by Yadhunandan and Anbazhagan (2026). The method uses a dynamic duration window defined by the first sign reversal in either force or velocity, as given in Eq. (2). A force reversal indicates a reflected tensile wave, while a velocity reversal marks a change in particle motion. This approach captures only the energy that contributes to sampler penetration, thereby reducing dependence on rod length-based theoretical cutoff durations and enabling estimation of ETR from the measured response. The method was experimentally validated through simultaneous force and velocity measurements together with independent high-speed camera observations of circular target marks in three dimensions, demonstrating that the selected cutoff accurately captures the energy that contributes to sampler penetration.

$$ETR(\%) = \frac{E_{FVCD}}{PE} * 100 = \frac{\int_{t=0}^{t=t_{FVCD}} F(t) * V(t)dt}{PE} * 100 \quad (2)$$

with

$t_{FVCD} = min(t_F, t_V)$

where: ETR = Energy Transfer Ratio (in %), E_{FVCD}= energy evaluated using the FVCD method (in Joules), PE= Potential energy of the hammer impact (in Joules), t_{FVCD}= dynamic cutoff time when force or velocity first changes sign from positive to negative, t_F= time of first sign reversal in force from positive to negative, t_V= time of first sign reversal in velocity from positive to negative, $t_{FVCD} = \min(t_F, t_V), F(t)$ = measured force at the anvil or sampler level (in N), and$V(t)$ = particle velocity obtained by integrating the measured acceleration (in m/s).

2.2. Instrumentation

The study utilized a custom-developed, simplified 2-channel system called SPT-HEMA (SPT – Hammer Energy Measurement Apparatus) (Anbazhagan et al., 2022b, 2021) and a commercially available 4-channel system. The SPT-HEMA consists of two instrumented rods connected to a Data Acquisition System (DAQ). Each rod carries a strain gauge and an accelerometer, providing two channels of data for measuring force and acceleration. The DAQ records at 60 kHz per channel, ensuring that high-frequency impact events are captured. Depending on accelerometer capacity, the system is referred to as 2C-5000g (2-channel rod with a 5000g accelerometer) or 2C-10000g (2-channel rod with a 10,000g accelerometer). Each load cell has a maximum capacity of 240 kN. Data were processed using MATLAB scripts, with ETR calculated by integrating the product of the measured force and velocity time histories, as described by the FVCD method (Eq. (2)). A key feature of the system is its ability to use two rods simultaneously, enabling measurements at both anvil and sampler levels. While anvil placement is conventional, sampler-level placement provides a more direct estimate of the penetration energy (Yadhunandan and Anbazhagan, 2025). The system is compact and designed for field use in boreholes 100–150 mm in diameter or above, and it functions reliably even in the presence of drill mud or groundwater.

To compare the performance of the 5000g and 10,000g accelerometers and the 2- and 4-channel rods, a commercial 4-channel system was used, hereafter referred to as 4C-10000g (4-channel rod with 10,000g accelerometers). The 4C-10000g incorporates dual strain gauges and dual accelerometers in a single rod, with a 240 kN load capacity and 10,000g acceleration capacity. The signals from the two strain gauges and two accelerometers are averaged, and the corresponding energy is subsequently calculated. This setup is designed exclusively for anvil-level measurements. In comparative setups, the 4C-10000g was placed directly below the anvil, with the custom 2C-5000g or 2C-10000g rod positioned beneath it in the drill rod assembly. The 2C-5000g/2C-10000g system additionally enabled energy measurement at the sampler level using a second instrumented rod installed above the sampler. Data from both systems were collected with their respective DAQs and processed in MATLAB and Excel for waveform and ETR analysis. Detailed waveform patterns, ETR results, and statistical agreement between the two systems are presented in later sections.

2.3. Laboratory experiments

To validate the performance of the different sensor configurations under repeatable conditions, the investigation began with a series of full-scale laboratory experiments. The controlled full-scale laboratory SPT model test setup was built within the existing building of the Soil Mechanics Laboratory, Civil Engineering department, at IISc, Bangalore. To facilitate SPT testing, 150 mm-diameter holes were cut into the floor slab, allowing SPT tests at various levels to simulate varying drill rod lengths and test depths. Fig. 1 provides a multi-perspective view of the laboratory SPT model setup. This includes an overhead layout, a close-up of the SPT instrumentation, and an overall front elevation view of the laboratory building. The soil cylinder consisted of a cylindrical acrylic confinement chamber, with a 500 mm internal diameter and 1000 mm height, supported on a steel base and externally reinforced by steel rings spaced at regular intervals for structural stability. The chamber was filled with sand prepared under controlled density conditions and used for the tests. The cylinder

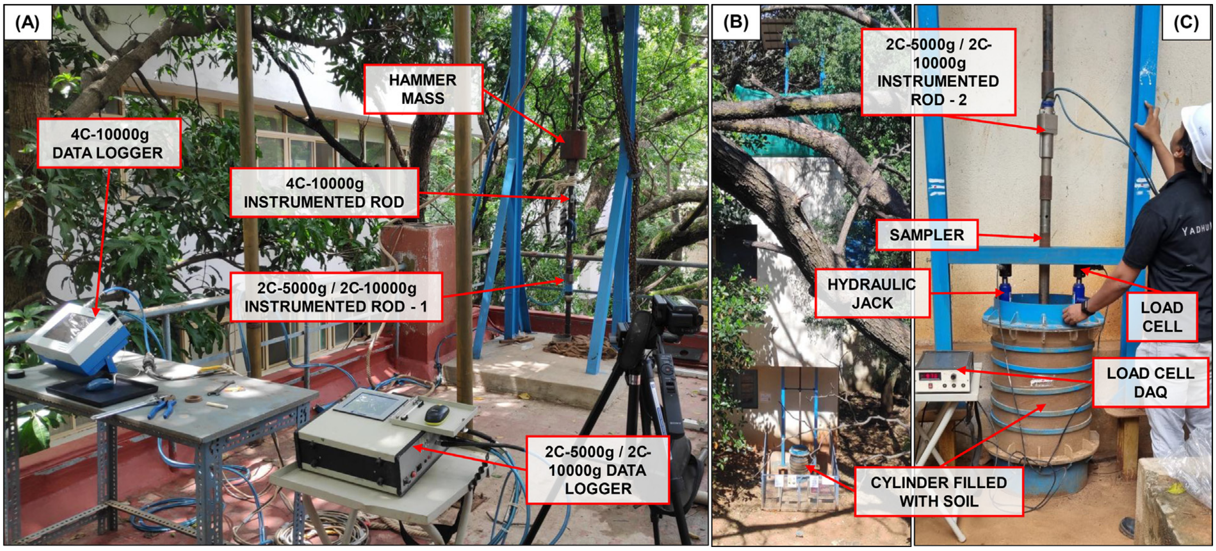

Fig. 1. Full-scale laboratory SPT hammer energy measurement setup at IISc using the 2C-5000g/2C-10000g (two instrumented rods) and 4C-10000g systems, shown from three perspectives: (A) terrace view with the hammer-drop system and instrumentation, (B) the overall front elevation of the building, and (C) the ground-level view of the soil cylinder with overburden loading arrangements.

diameter (500 mm) was selected to provide sufficient lateral confinement relative to the sampler diameter, thereby minimizing boundary effects and energy dissipation. Sand was placed in 5–10 layers using controlled height-of-fall and tamping methods to achieve the target relative density. For higher densities (greater than 65% relative density), a mechanical vibrator was additionally used to ensure uniform compaction. The test setup included the provision to apply overburden pressure to the soil sample to simulate field conditions. A 6 mm-thick mild steel annular plate (outer diameter 498 mm, central opening 150 mm) was placed at the top of the soil surface to simulate a standard borehole diameter typically used in SPT testing (100–200 mm). Vertical overburden pressure was applied using two 5-tonne hydraulic jacks equipped with 100 kPa load cells to replicate field stress conditions. A more detailed description of the experimental methodology, instrumentation, and test procedures is presented by Yadhunandan and

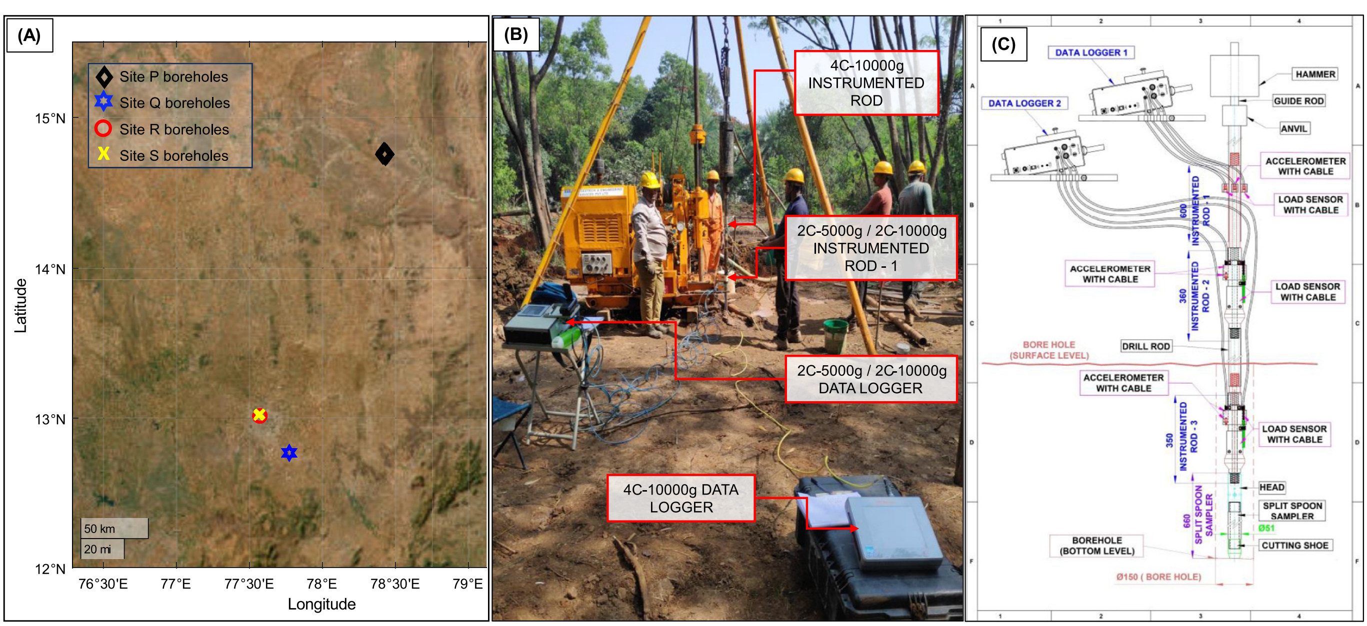

Fig. 2. Field SPT setup: [A] Test locations of boreholes across Sites P, Q, R and S, [B] Typical SPT hammer energy measurement using 2C-5000g/2C-10000g (two instrumented rods) and 4C-10000g systems with their respective data loggers, and [C] Schematic diagram illustrating the three instrumented rods with their respective data loggers and the installation positions of the accelerometers and load sensors at the anvil and sampler levels within the SPT assembly.

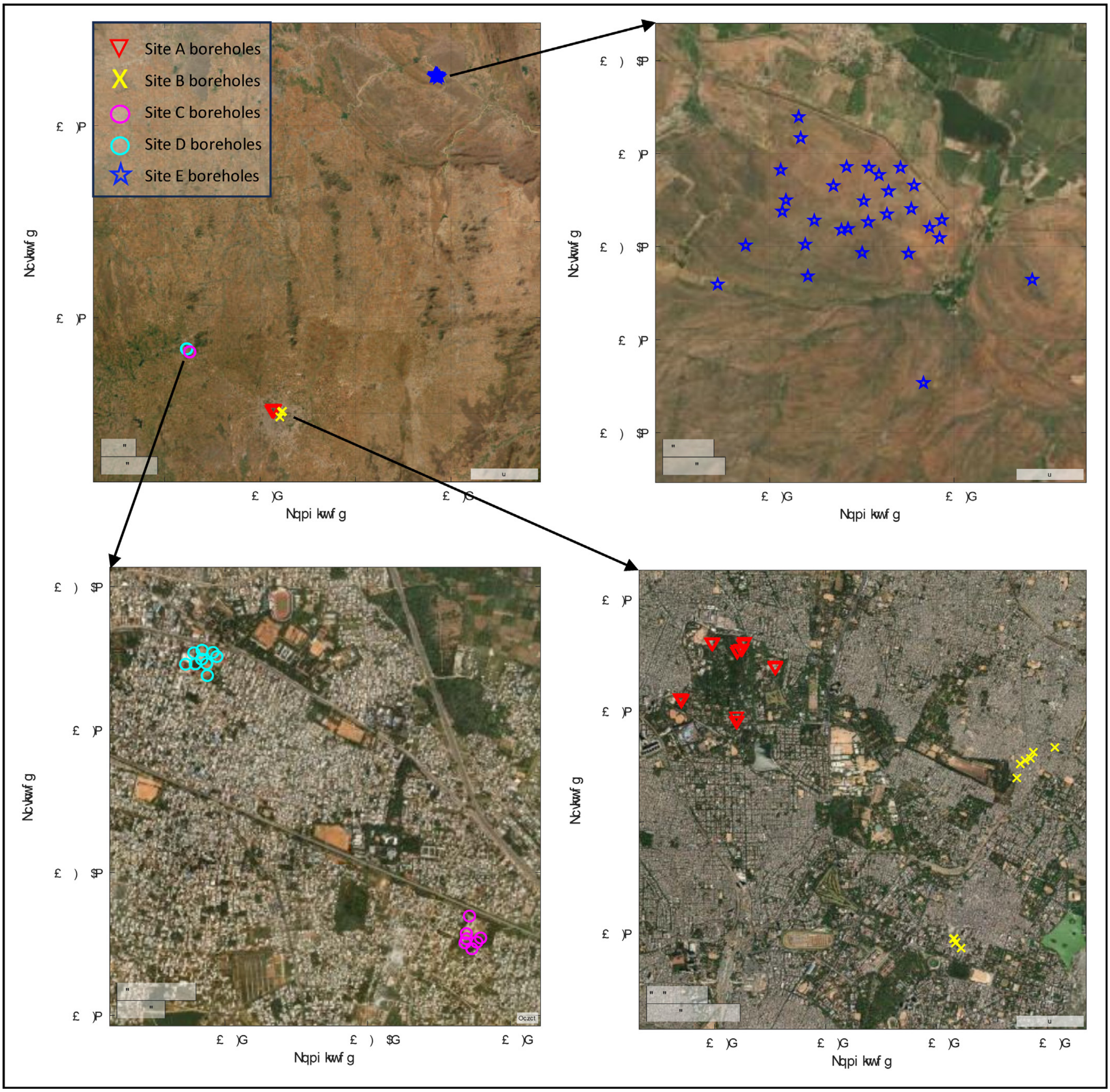

Fig. 3. Test locations of SPT energy measurement using the 2C-10000g system (two instrumented rods).

Anbazhagan (2025). The hammer energy measurements were conducted using the 2C-5000g, 2C-10000g, and 4C-10000g configurations.

2.4. Field experiments

After completing the laboratory tests, field studies were conducted at multiple locations to evaluate system performance under real-world site conditions. Figs. 2 and 3 collectively illustrate the spatial extent and field instrumentation setup employed in this study for SPT hammer energy measurement using the custom-developed systems (2C-5000g/2C-10000g) and the commercial system (4C-10000g). Fig. 2(A) presents the geographical locations of four key test sites: Site P to Site S. Simultaneous measurements were carried out using both systems. The distribution of boreholes across these sites, marked with distinct symbols, demonstrates broad spatial coverage and reinforces the study's focus on capturing energy-transfer variability across varying field conditions and equipment setups. Fig. 2(B) depicts a typical field deployment showing both the 2C-5000g/2C-10000g and the 4C-10000g systems in operation. The setup includes two instrumented rods for the 2C-5000g/2C-10000g (one of which is visible at anvil level in the image; also called the top instrumented rod), along with separate data loggers for each system. This visual documentation confirms the dual-instrumentation methodology and underscores the feasibility of a real-time, side-by-side comparison between the two systems under field conditions. Fig. 2(C) provides a schematic overview of the instrumentation layout and corresponding data loggers, clearly indicating the positions of accelerometers and load sensors installed on the three instrumented rods at the anvil and sampler levels within the SPT assembly. This schematic clarifies the sensor arrangement and measurement levels adopted in the study. Fig. 3 expands the scope of the investigation by showing five additional sites: Site A to Site E. The energy measurements were performed exclusively with the 2C-10000g system (two instrumented rods). The regional map in the upper-left corner offers a macro view of the site locations, while the accompanying zoomed-in panels reveal the detailed borehole layouts within each site. Symbols such as red triangles, yellow crosses, magenta circles, cyan ovals, and blue stars denote the boreholes associated with Sites A to E, respectively.

Table 1 presents the stratigraphic profiles and soil classifications encountered at the various field study sites, offering essential context for interpreting the ETR variability observed during the SPT. The recorded data categorize soil types at 2-m depth intervals to show vertical consistency and to reflect the typical SPT test interval of 1–1.5 m. Empty cells in the table indicate that no soil description was available at the corresponding depth due to non-recovery, rebound, rock drilling, SPT not being performed, or borehole termination. The soil at these sites exhibited limited stratigraphic variability across boreholes, ensuring a relatively uniform soil profile for all tests. This consistency in soil conditions serves as a significant factor in the study and allowed the effects of different drilling rigs, hammer mechanisms, and SPT components on the ETR measurements to be isolated, as all tests were conducted under the same supervision and climatic conditions.

2.5. Test in diverse rigs and hammer-drop mechanisms

Fig. 4 illustrates the diversity of drilling rigs and hammer-drop mechanisms used during SPT hammer energy measurements. Each setup represents a unique configuration commonly encountered in field conditions. The panels illustrate five different configurations: [A] RMH – Rotary drill rig with a manual rope and pulley system for lifting the hammer; [B] RSH – Rotary drill rig using a spool winch for manual or semi-mechanical hammer lifting; [C] HSH – Hydraulic drill rig with a spool winch-operated hammer; [D] HTH – Hydraulic drill rig equipped with an auto trip hammer system; and [E] MAH – Multipurpose drill rig using a fully automated hammer system. Each rig setup exhibits distinct differences in SPT components, including the hammer shape, drop mechanism, anvil type, drill rod dimensions, and other related components. The hammer's physical dimensions and geometry vary significantly, which can influence impact efficiency and energy transmission. Similarly, the anvil size, rod alignment, and verticality also differ across setups, introducing additional variability and potential sources of energy loss or measurement error.

In continuation of the rig illustrations shown in Fig. 4, Table 2 presents detailed specifications of the various SPT rigs used in this study. It includes important SPT component properties such as hammer diameter, height, and weight; anvil type and dimensions; drill rod type; and the number of boreholes and blows recorded for each rig. Even though the nominal hammer weight is around 63.5 kg for all rigs, Table 2 clearly shows that the hammer geometry, anvil type (plate, coupler, or cylinder), and drill rod configurations vary significantly across rigs and sites. This highlights the non-standardized nature of field SPT practices, reinforcing the core argument of this study that, due to inherent variability in equipment, even under similar soil conditions, the standard assumptions about uniform energy transfer may not hold across different rigs and hammer-drop mechanisms. These findings highlight the value of energy measurement in improving the reliability and consistency of SPT N-value interpretation. The energy variability among the rigs is explained in the following sections.

3. Results and Discussion

A total of 314 field SPT tests (20,448 blows) and 42 laboratory SPT tests (821 blows) were analyzed using two systems, 2C-5000g/2C-10000g and the 4C-10000g systems. One part of the study aimed at evaluating the performance of 2-channel versus 4-channel setups and the accuracy of the 5000g versus 10,000g accelerometers. This was achieved by comparing results from both systems at selected test sites (Sites P to S) and under laboratory conditions. After establishing the sufficiency of the 2-channel system, the 2C-10000g system was used to examine the detailed ETR variations across different rigs and soil conditions at five additional sites (Sites A–E). These sites were chosen for their geotechnically similar soil profiles within the same project area, allowing the evaluation of how different rigs perform under consistent soil conditions and how equipment variability affects ETR. The results are discussed across five major themes, covering waveform comparisons, ETR distribution, laboratory and field test validation, and rig-wise variability, as presented in the following sections.

3.1. Waveform comparison across sensor configurations

This section compares the waveforms recorded by the 4C-10000g and 2C-5000g/2C-10000g systems for a single SPT hammer blow. Figs. 5 and 6 illustrate the performance of different sensor setups. Fig. 5 presents results from the 2C-5000g setup, while Fig. 6 presents results from the

Table 1
Soil profiles at study locations at 2 m depth intervals. Sites P-S correspond to Phase I, while Sites A-E correspond to Phase II.

Soil profile	**Test location**								
	Site P	**Site Q**	**Site R**	**Site S**	**Site A**	**Site B**	**Site C**	**Site D**	**Site E**
0–2 m	Weathered Rock	Silty Clay & Clayey Sand	Sandy Clay	–	Clayey silt & Clayey Sand	Sandy Silt & Silt	Sandy Silt & Silty Sand	–	Weathered Rock& Sandy Gravel
2–4 m	–	Silty Clay & Sandy Clay	Sandy Silt	Clayey Silt	Clayey silt & Silty Clay	Sandy Silt & Silt	Silty Sand & Sandy Silt	Clayey Silt & Silty Sand	–
4–6 m	–	Silty Clay & Sandy Silt	Sandy Silt	Clayey Silt	Silty Sand & Sandy Silt	Silt & Clayey Silt	Sandy Silt & Silty Sand	Clayey Silt & Gravelly Silt	–
6–8 m	–	Silty Sand & Clayey Sand	Silty Sand	Sandy Silt	Silty Sand & Sandy Silt	Clayey Silt & Sandy Silt	Silty Sand & Sandy Silt	Gravelly Silt & Silt	–
8–10 m	–	Silty Sand & Sandy Gravel	Silty Sand	–	Silty Sand & Weathered Rock	Clayey Silt & Silt	Silty Sand & Sandy Silt	Gravelly Silt	–
10–12 m	–	Gravelly Sand & Sandy Gravel	Silty Sand	–	Silty Sand & Sandy Silt	Silty Sand & Sandy Silt	Silty Sand & Sandy Silt		–
12–14 m	–	–	–	–	Sandy Silt & Silty Sand	Silty Sand & Weathered Rock	Silty Sand		–
14–16 m	–	–	–	–	Sandy Silt & Silty Sand	Weathered Rock & Silt			–
16–18 m	–	–	–	–	Silty Sand & Sandy Silt	Weathered Rock & Sandy Silt			–
18–20 m	–	–	–	–	Silty Sand & Sandy Gravel	–			–
20–22 m	–	–	–	–	Silty Sand	Weathered Rock		–	–
22–24 m	–	–	–	–	Silty Sand			–	–
24–26 m	–	–	–	–	Silty Sand			–	–
26–28 m	–	–	–	–	Silty Sand			–	–
28–30 m	–	–	–	–	Silty Sand		–	–	–

Note: "-" indicates that no soil description was available at the corresponding depth due to non-recovery, rebound, rock drilling, SPT not being performed, or borehole termination.

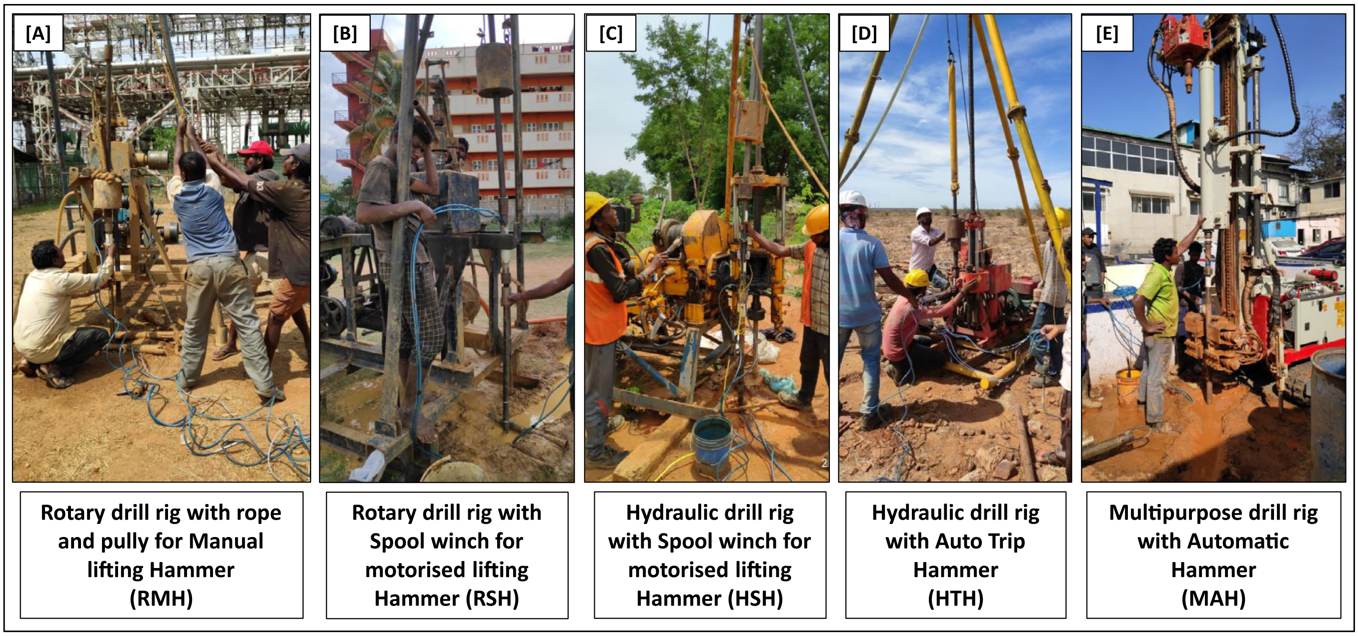

Fig. 4. SPT hammer energy measurement setups showing diverse rigs and hammer-drop mechanisms. Additionally, the figure highlights different SPT components, including hammer and anvil dimensions. [A] Rotary drill rig with rope and pulley for Manual lifting Hammer (RMH); [B] Rotary drill rig with Spool winch for motorized lifting Hammer (RSH); [C] Hydraulic drill rig with Spool winch for motorized lifting Hammer (HSH); [D] Hydraulic drill rig with Auto Trip Hammer (HTH); [E] Multipurpose drill rig with Automatic Hammer (MAH).

2C-10000g setup. Each figure includes four plots: acceleration, force, velocity, and ETR over time. The acceleration plots (A) show a sharp initial spike followed by smaller vibrations, captured similarly by both systems. The force plots (B) also align well, confirming that both instruments effectively measure the hammer impact force. Similar waveform behaviour is consistent with earlier instrumented rod studies (Howie et al., 2003; Lukiantchuki et al., 2017; Odebrecht et al., 2005), where acceleration and force signals showed sharp initial peaks followed by secondary oscillations. In the velocity plots (C), the curves follow nearly identical patterns, particularly at the start of the impact when energy transmission is significant. The ETR plots (D) show energy build-up over time, eventually stabilizing at approximately 54% for the 2C-5000g system (Fig. 5) and 64% for the 2C-10000g system (Fig. 6).

It should be noted that the comparison between the 2-channel and 4-channel systems has an inherent experimental limitation arising from the sensor installation arrangement. Since both instrumented rods could not be installed at the identical measurement location simultaneously, the 4C-10000g rod was positioned immediately below the anvil, while the 2C-5000g/2C-10000g rod was installed directly beneath it. Consequently, the two systems recorded stress waves at slightly different locations along the drill rod, where minor attenuation and propagation effects may occur before the waves reach the lower instrumented rod. Therefore, small differences in the measured waveforms and ETR values are expected. The close agreement observed in both laboratory and field comparisons, together with the Bland-Altman analysis and ETR differences generally within ±5%, indicates that the sensor installation position has a relatively small influence and does not affect the overall conclusions of the present study. Nevertheless, the overall waveform comparisons show that the simpler 2C-5000g/2C-10000g system can reliably capture the SPT dynamic response and provides a practical alternative to the 4C-10000g system.

3.2. ETR distribution within a single SPT test

Next, the variation in hammer energy transfer from blow to blow within a single SPT test is analyzed to understand the consistency of energy delivery during the successive blows over the 30 cm penetration depth (i.e., the depth corresponding to an N-value). Fig. 7 shows the ETR for every individual blow recorded at one SPT test depth. Each blow is measured using three instrumented rods: the top instrumented rod of the 2C-5000g/2C-10000g and 4C-10000g systems, and the bottom instrumented rod of the 2C-5000g/2C-10000g system. Fig. 7A compares the data from the 2C-5000g and 4C-10000g systems, whereas Fig. 7B compares the data from the 2C-10000g and 4C-10000g systems. Despite using different sensor configurations at the anvil level, the ETR trends from both systems follow a very similar pattern, with only minor variations from blow to blow. This shows that even though all hammer blows may appear the same in the field, the energy actually delivered can differ slightly due to factors such as friction, rod alignment, or equipment variability, as reported in previous field investigations (Matsumoto et al., 2015; Sumanth et al., 2022). Nevertheless, the close

Table 2
Comparison of SPT component properties for different rigs at the same test site with uniform soil properties in this study.

Test Location	Location Radius (m) covering all Boreholes	Rig Type	Number of boreholes per Rig	Total Number of SPT	Total Blows	Hammer diameter (mm)	Hammer height (mm)	Hammer inner hole diameter (mm)	Anvil type	Anvil diameter (mm)	Anvil height (mm)	Rod type	Anvil weight (kg)	Hammer weight (kg) Measured
Site A	700	HTH_1	8	49	2820	200	263	29	Plate	200	40	AW	9.9	63.5
		HSH_1	6	50	2985	200	260	30	Plate	200	40	AW	9.9	63.0
		RMH_1	2	11	427	197	286	46	Coupler	52	72	Calyx	1.2	65.0
		HSH_2	2	15	714	192	295	48	Cylinder	83	96	AW	4.1	63.6
		RSH_1	2	11	623	207	255	48	plate	115	9	NW	0.7	64.1
		HSH_3	2	10	478	187	318	51	Cylinder	103	111	AW	7.3	64.0
		HSH_4	3	12	538	184	318	50	Cylinder	88	101	AW	4.6	62.0
		RSH_2	1	7	373	207	240	46	Coupler	46	98	BW	1.3	61.3
Site B	1000	HSH_5	3	6	216	201	259	52	Cylinder	96	117	AW	6.6	63.9
		HTH_2	3	6	370	200	272	50	Cylinder	82	97	AW	4.0	64.0
		MAH_1	5	35	602	100			ball head	60	120	1.4 × AW	2.7	63.5
Site C	130	RMH_2	5	24	1739	201	259	46	Coupler	54	58	Calyx	1.0	62.0
		RMH_3	4	30	4570	210	253	55	Cylinder	104	109	NW	7.3	64.5
Site D	170	RMH_4	4	13	1644	201	259	46	Coupler	54	58	Calyx	1.0	62.0
		RMH_5	3	8	1380	210	253	55	Cylinder	104	109	NW	7.3	64.5
Site E	500	RMH_6	12	15	462	213	239	48	Cylinder	89	124	AW	6.1	65.0
		HTH_3	12	12	507	203	273	60	Cylinder	121	140	AW	12.6	63.5

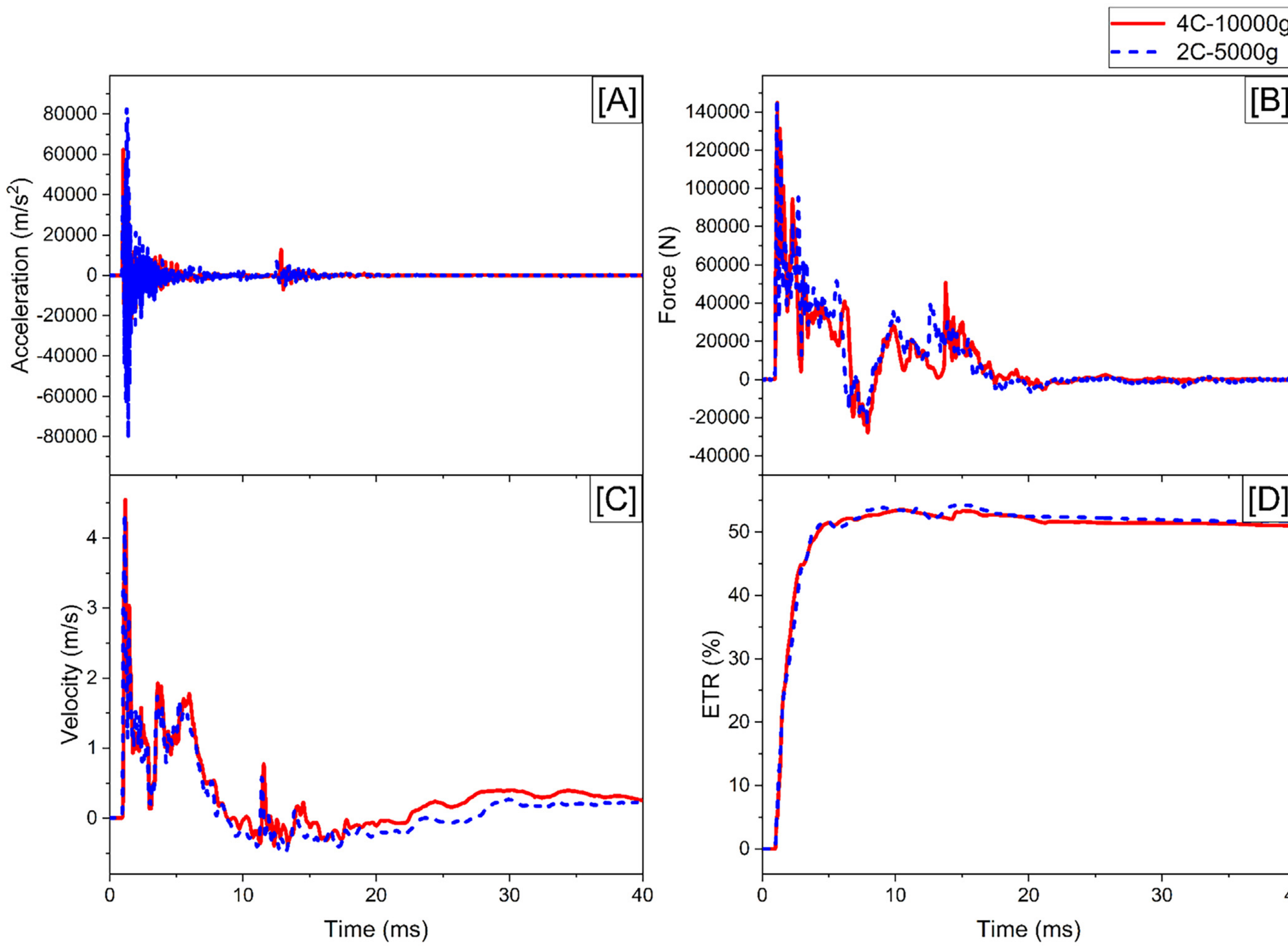

Fig. 5. Comparison of typical time-history plots between a 4C-10000g system and a 2C-5000g system:(A) Acceleration, (B) Force, (C) Velocity, and (D) ETR.

match between the two systems confirms that the 2C-5000g/2C-10000g system performs consistently across different sensor capacities. Additionally, these results demonstrate the value of blow-wise energy measurements for investigating blow-by-blow variability, particularly where high-accuracy energy correction is required. Furthermore, instrumented rods positioned at the anvil level typically record higher ETR values than those at the sampler level, highlighting energy loss along the drill rods. This indicates that such losses are unavoidable under real-world testing conditions and that measuring energy at the sampler level offers a more accurate estimate of the energy effectively transmitted to the sampler during penetration (Yadhunandan and Anbazhagan, 2025).

3.3. ETR comparison across large datasets

To further validate the sensor configurations under controlled conditions, a series of laboratory tests was conducted to compare ETR measurements from both systems. The comparison of ETR results from controlled laboratory SPT tests is shown in Figs. 8 and 9. In both figures, plot (a) shows the average ETR (%) for each test with standard deviation error bars, while plot (b) presents the Bland-Altman plot to assess the agreement between the two systems. Fig. 8 compares the 2C-5000g system against the 4C-10000g system, whereas Fig. 9 compares the 2C-10000g and 4C-10000g systems. Across the tests, the ETR values from both systems show similar trends, with only slight differences.

The Bland-Altman plots in plot (b) visualize these differences more clearly. The x-axis shows the average ETR, while the y-axis shows the difference between the two systems. The mean difference (bias) is −1.76% for Fig. 8 and −2.11% for Fig. 9, indicating that the 2C-5000g/2C-10000g measurements were slightly lower on average. The limits of agreement (mean ± 1.96 × SD) range from −5.79% to +2.28% in Fig. 8 and −6.06% to +1.83% in Fig. 9. Most data points lie within these limits, indicating good agreement in both configurations. These small variations are likely due to the physical placement of the sensor, where one instrumented rod was mounted just below the other, as well as minor energy losses along the rods. Similar agreement levels between different instrumentation systems

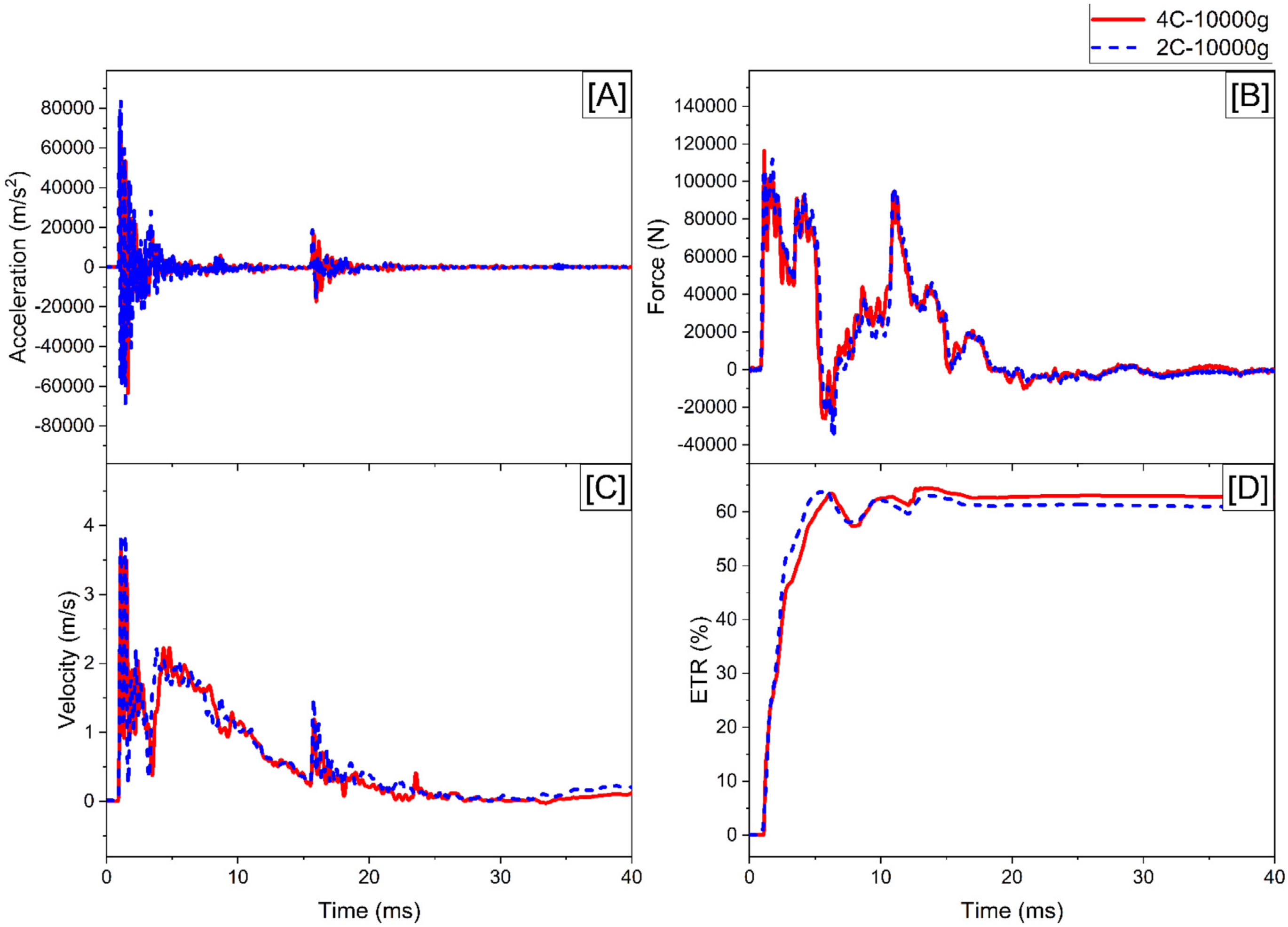

Fig. 6. Comparison of typical time-history plots between a 4C-10000g system and a 2C-10000g system: (A) Acceleration, (B) Force, (C) Velocity, and (D) ETR.

have been reported in previous comparative studies of SPT energy measurement systems (Anbazhagan et al., 2022b; Hong et al., 2022). Overall, both figures confirm that the simpler, more flexible 2C-5000g/2C-10000g system yields ETR results that closely match those of the 4C-10000g system.

In continuation of the laboratory test comparisons, field SPT tests were also conducted to evaluate the sensor performance of the two systems under real-world conditions. The comparison is shown in Figs. 10 and 11, and a similarly good agreement was observed with the laboratory comparison. The ETR values from both systems are closely aligned across a wide range of depths, boreholes, and sites, with consistent overall trends. This indicates that both systems produce similar ETR values in the field. While minor differences are visible in some locations, the overall trends remain consistent. The Bland-Altman plots show a mean difference of −0.71% for the 2C-5000g system (Fig. 10) and −0.76% for the 2C-10000g system (Fig. 11). These narrow ranges and centered bias lines suggest good agreement between the systems, with most points falling within the shaded bands. Despite site variability and field-specific factors, the differences between the systems remain small and consistent.

The results presented in Table 3 provide a statistical summary of the ETR values measured using both the 4C-10000g and 2C-5000g/2C-10000g systems across the controlled laboratory setup and four field sites (P, Q, R, and S). For each location, the average ETR and its standard deviation (SD) are shown, allowing a direct comparison of system performance. The values recorded by both systems are closely matched, indicating good agreement. For instance, in the laboratory tests, the 4C-10000g system measured an average ETR of 58.91% (±7.33), while the 2C-5000g/2C-10000g system measured 55.87% (±9.43). Similarly, at Site P, the values were 73.25% (±7.27) and 72.57% (±8.26), and at Site Q, they were 39.06% (±3.38) and 38.28% (±3.77) for the 4C-10000g and 2C-5000g/2C-10000g systems, respectively. Even at Site S, where slightly higher variability was observed, the results remained consistent, with only a small difference in average values. In both laboratory and field results, most values fall within ±5% of each other. Together, these results confirm that the 2C-5000g/2C-10000g system provides reliable ETR

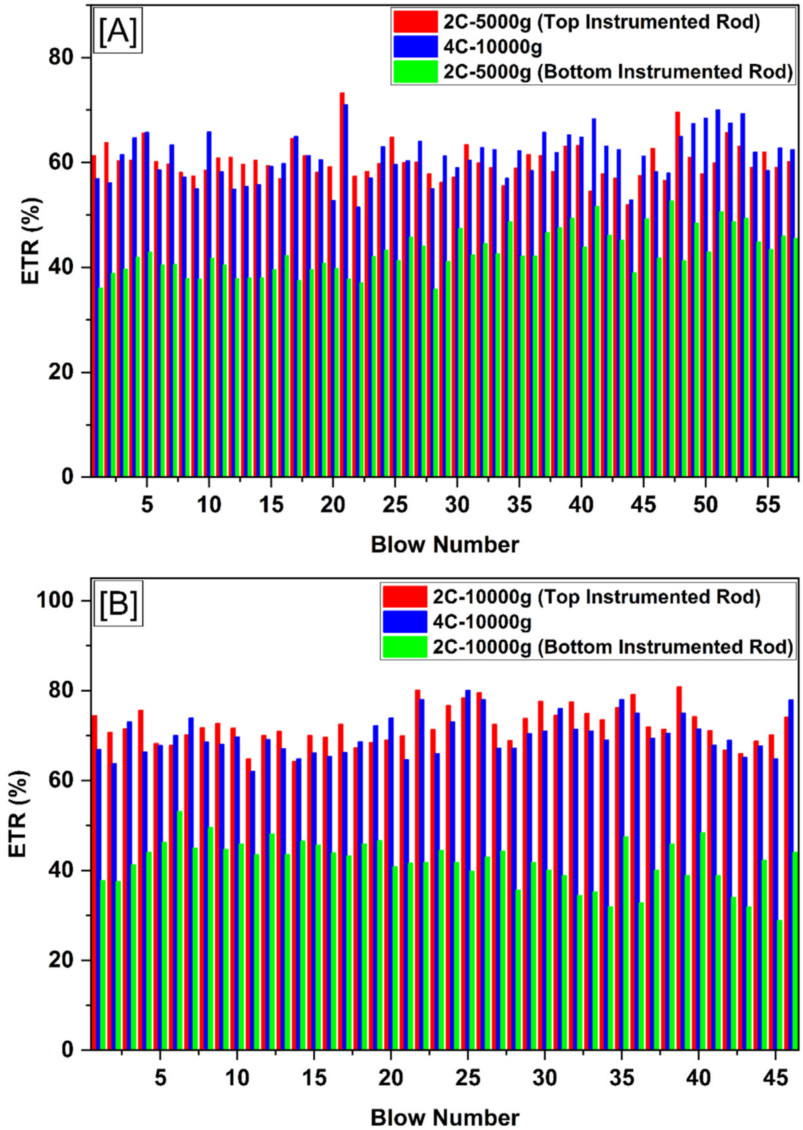

Fig. 7. Blow-by-blow comparison of ETR (%) during a single SPT test using [A] two 2C-5000g systems and a 4C-10000g system; [B] two 2C-10000g systems and a 4C-10000g system.

measurements in both laboratory and field conditions. Its consistent performance across different rigs and setups demonstrates that the 2C-5000g/2C-10000g configuration is a simpler, more affordable system, and is well-suited for routine field use and large-scale geotechnical projects.

3.4. ETR variation across multiple rigs within the same test site and project

After evaluating the performance of different sensor configurations under both laboratory and field conditions, a critical analysis was conducted to compare the energy variability within individual boreholes for different drill rigs using the 2C-10000g setups. Figs. 12 and 13 present the depth-wise variation of ETR at the anvil and sampler levels, respectively, across five boreholes drilled using different rigs: [A] RMH, [B] RSH, [C] HSH, [D] HTH, and [E] MAH. In addition to individual depth measurements (with error bars), the plots show 3-depth, 5-depth, and all-depth average trends to assess the validity of common ETR assumption practices on large projects. The error bars shown in Figs. 12 and 13 represent ±1 SD of the blow-wise ETR values recorded at each specific test depth, thereby reflecting the variability of energy delivery within each SPT test depth.

A detailed examination of the Anvil ETR (Fig. 12) reveals two critical findings. Firstly, there is a substantial variation in the mean ETR delivered by different rigs, ranging from a high of ~85.4% for the MAH rig (Fig. 12[E]) to a low of ~45.2% for the HSH rig (Fig. 12[C]). Secondly, there is a significant difference in the consistency of energy delivery. The automatic hammer systems, HTH (Fig. 12[D]) and MAH (Fig. 12[E]), exhibit good consistency with

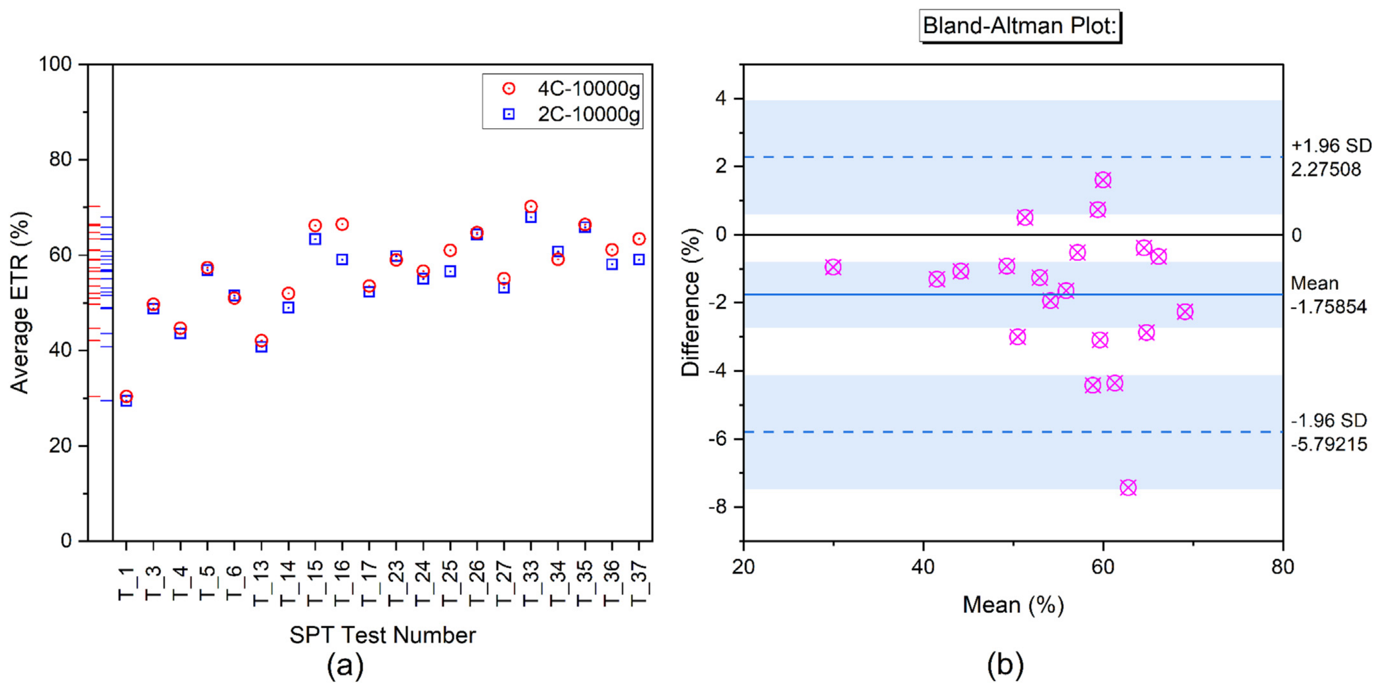

Fig. 8. Comparison between the 2C-5000g and 4C-10000g systems in controlled laboratory SPT tests: (a) average ETR (%) with SD error bars, and (b) Bland-Altman plot showing agreement between the two systems.

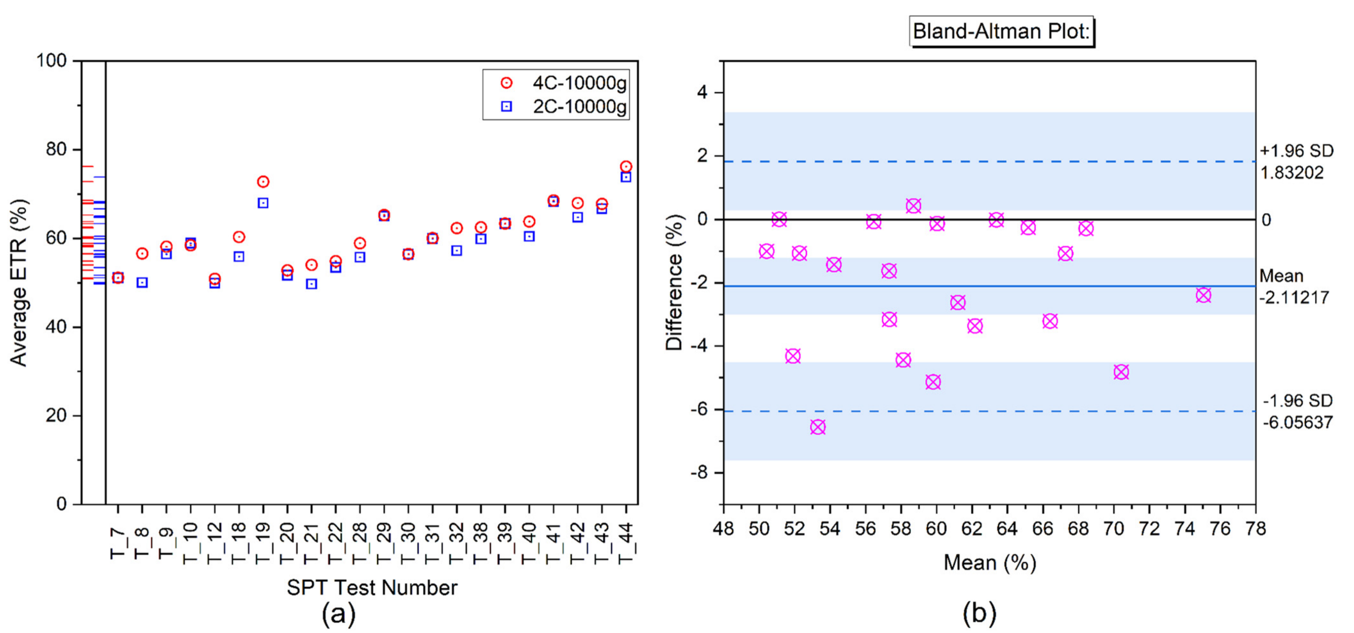

Fig. 9. Comparison between the 2C-10000g and 4C-10000g systems in controlled laboratory SPT tests: (a) average ETR (%) with SD error bars, and (b) Bland-Altman plot showing agreement between the two systems.

depth, characterized by shorter error bars and consistent ETR values. In contrast, the RSH rig (Fig. 12[B]) shows considerable variability, with the Anvil ETR dropping from ~98% at 2 m to ~60% at 6 m. This high variation demonstrates that, for such systems, using a simplified average ETR (3-, 5-, or all-depth average) instead of measuring at every SPT depth can be highly misleading and may fail to represent the actual energy delivered at any given SPT depth. For instance, in the RSH rig (Fig. 12 [B]), the 'all-depth average' is approximately 80%, yet this single value completely masks the measured peak ETR of nearly 98% at 2 m and the subsequent drop to around

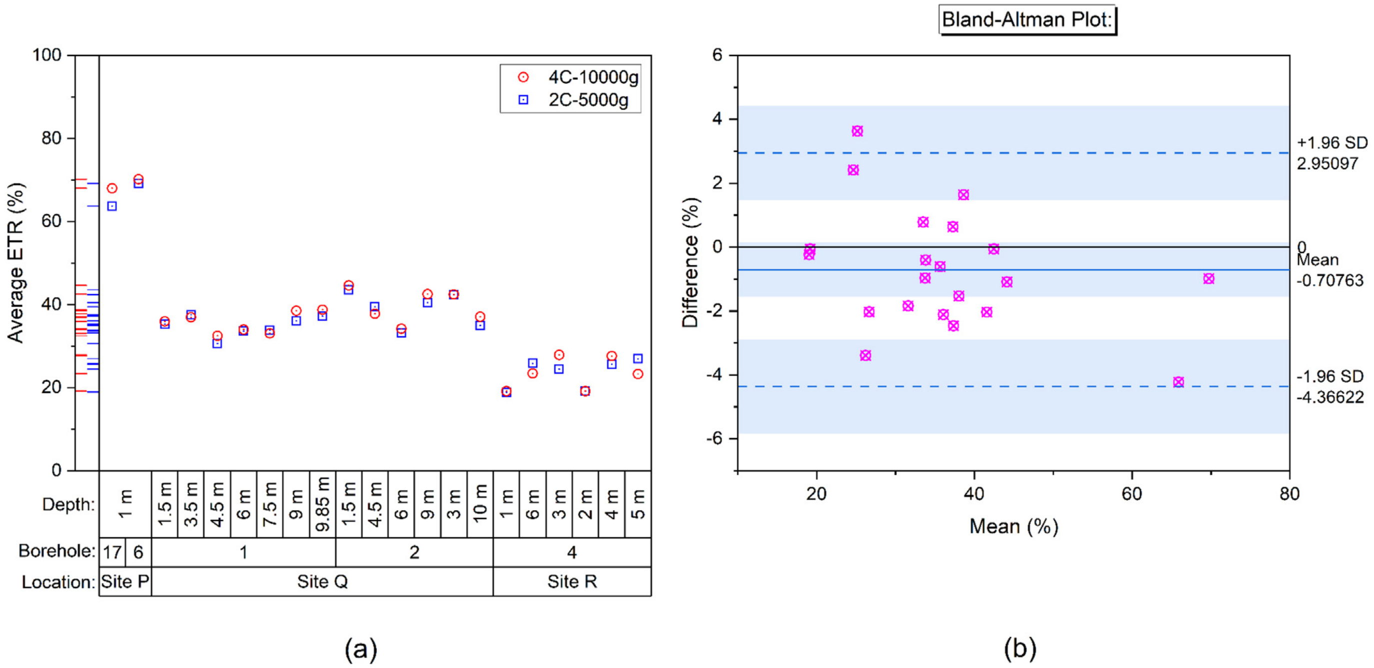

Fig. 10. Comparison between the 2C-5000g and 4C-10000g systems in field SPT tests: (a) average ETR (%) with SD error bars, and (b) Bland-Altman plot showing agreement between the two systems.

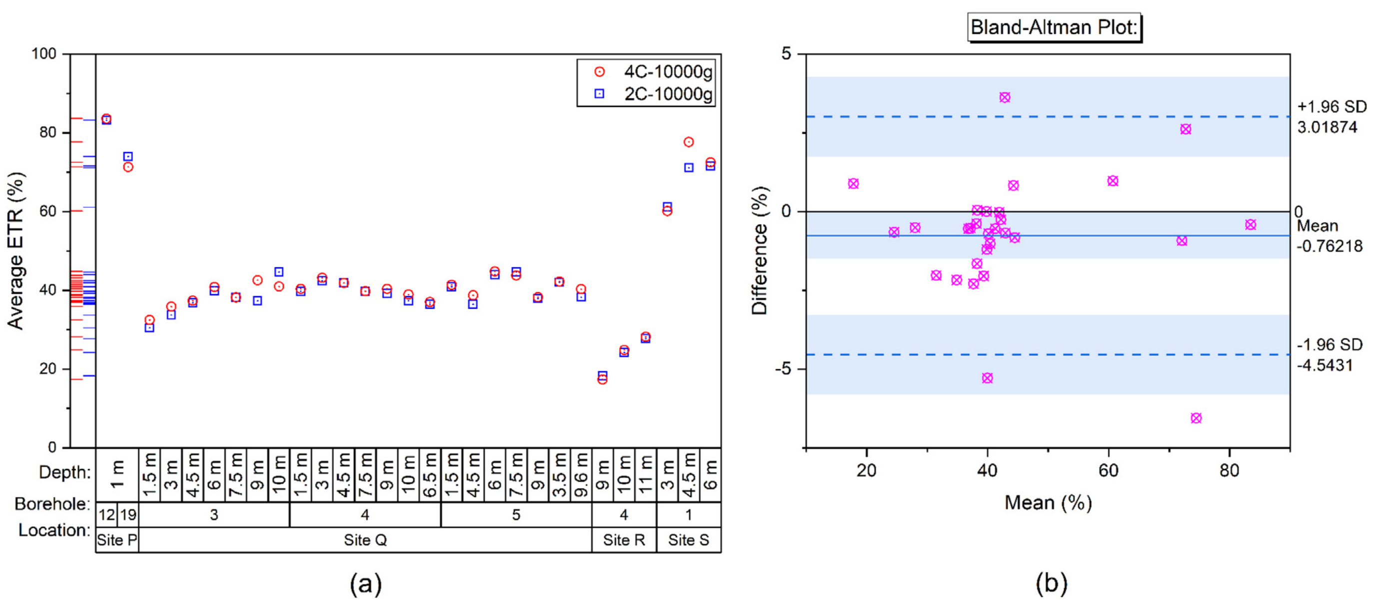

Fig. 11. Comparison between the 2C-10000g and 4C-10000g systems in field SPT tests: (a) average ETR (%) with SD error bars, and (b) Bland-Altman plot showing agreement between the two systems.

60% at 6 m. The moving averages also smooth out these sharp fluctuations, ultimately failing to represent the actual, highly variable energy delivered during a specific test.

Similar trends are observed at the sampler level (Fig. 13), although overall ETR values are lower due to energy dissipation along the drill rods. The MAH (Fig. 13[E]) and RSH (Fig. 13[B]) rigs again record the highest average Sampler ETRs (~49.6% and ~51.3%), while the HSH rig (Fig. 13[C]) remains the poorest performer at ~21.1%. The significant variability of rigs like RSH (Fig. 13[B]) persists at the sampler, confirming that inconsistent energy delivery is a characteristic of the hammer system. For instance, in a borehole (Fig. 13[C]), the Sampler ETR varies from ~28% to as low as ~10%, with large error margins. Relying on a single average ETR in such cases can lead to significant errors when calculating the corrected N-value.

Table 3
Comparison of average ETR (%) and SD measured using the 4C-10000g and 2C-5000g/2C-10000g systems across laboratory and field test sites (P, Q, R, and S).

Test location	Average ETR and SD (%)	
	4C-10000g	2C-5000g/2C-10000g
SPT Lab Setup	58.91 ± 7.33	55.87 ± 9.43
Site P	73.25 ± 7.27	72.57 ± 8.26
Site Q	39.06 ± 3.38	38.28 ± 3.77
Site R	23.45 ± 4.13	23.47 ± 3.69
Site S	70.15 ± 9.00	67.99 ± 5.90

These findings clearly demonstrate the influence of rig-specific dynamics on energy delivery and underscore the importance of conducting full-depth ETR measurements to accurately correct SPT results. Consequently, such simplifications can lead to inaccurate energy corrections and the misinterpretation of SPT N-values. The large error margins further complicate the reliability of individual point measurements, highlighting the benefit of more comprehensive full-depth energy monitoring and more robust averaging strategies that account for uncertainty, rather than assuming uniform energy delivery across the test depth.

After evaluating the energy variability within individual boreholes for different drill rigs, the next step was to examine how energy transfer varied across multiple rigs operating within the same project site under uniform soil conditions. The test sites (A to E, as given in Table 2) were selected based on uniform soil layers and conditions within a limited radius (130 m to 1000 m), allowing a fair comparison across rigs. Multiple SPT rigs with varied hammer-drop mechanisms, including manual, semi-mechanical, hydraulic, and automatic systems, were used at each site under the same project supervision. This ensured that the differences observed in ETR values could be attributed mainly to the rigs, equipment, and SPT components, rather than soil or operator variability.

Figs. 14–19 collectively illustrate the variation of anvil-level and sampler-level ETR (%) across multiple rigs,

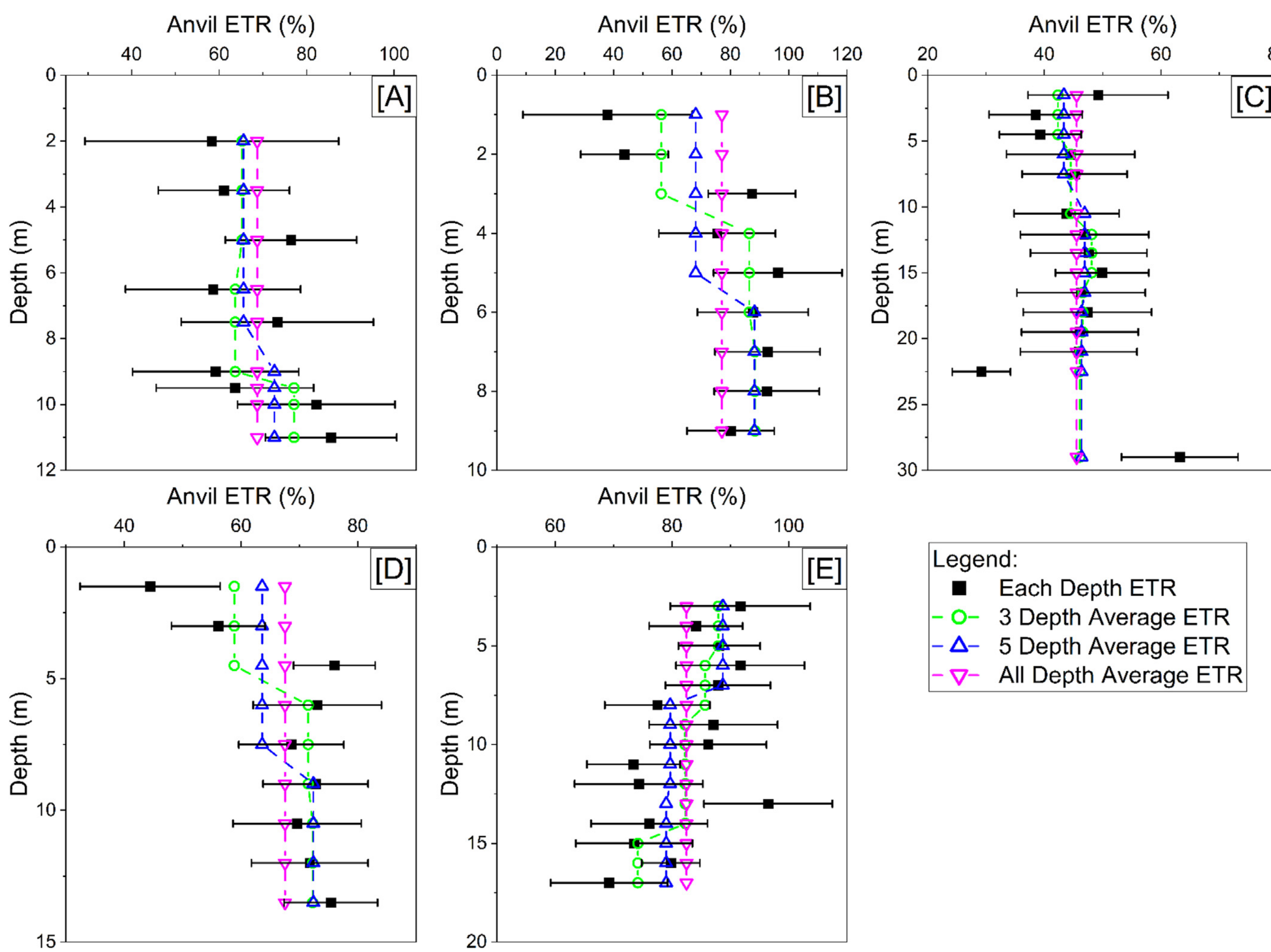

Fig. 12. Borehole-wise comparison of Anvil ETR (%) across different rigs: [A] RMH, [B] RSH, [C] HSH, [D] HTH, and [E] MAH; showing individual depth ETR values with error bars representing SD of blow-wise ETR measurements, along with 3-depth, 5-depth, and all-depth average ETR trend.

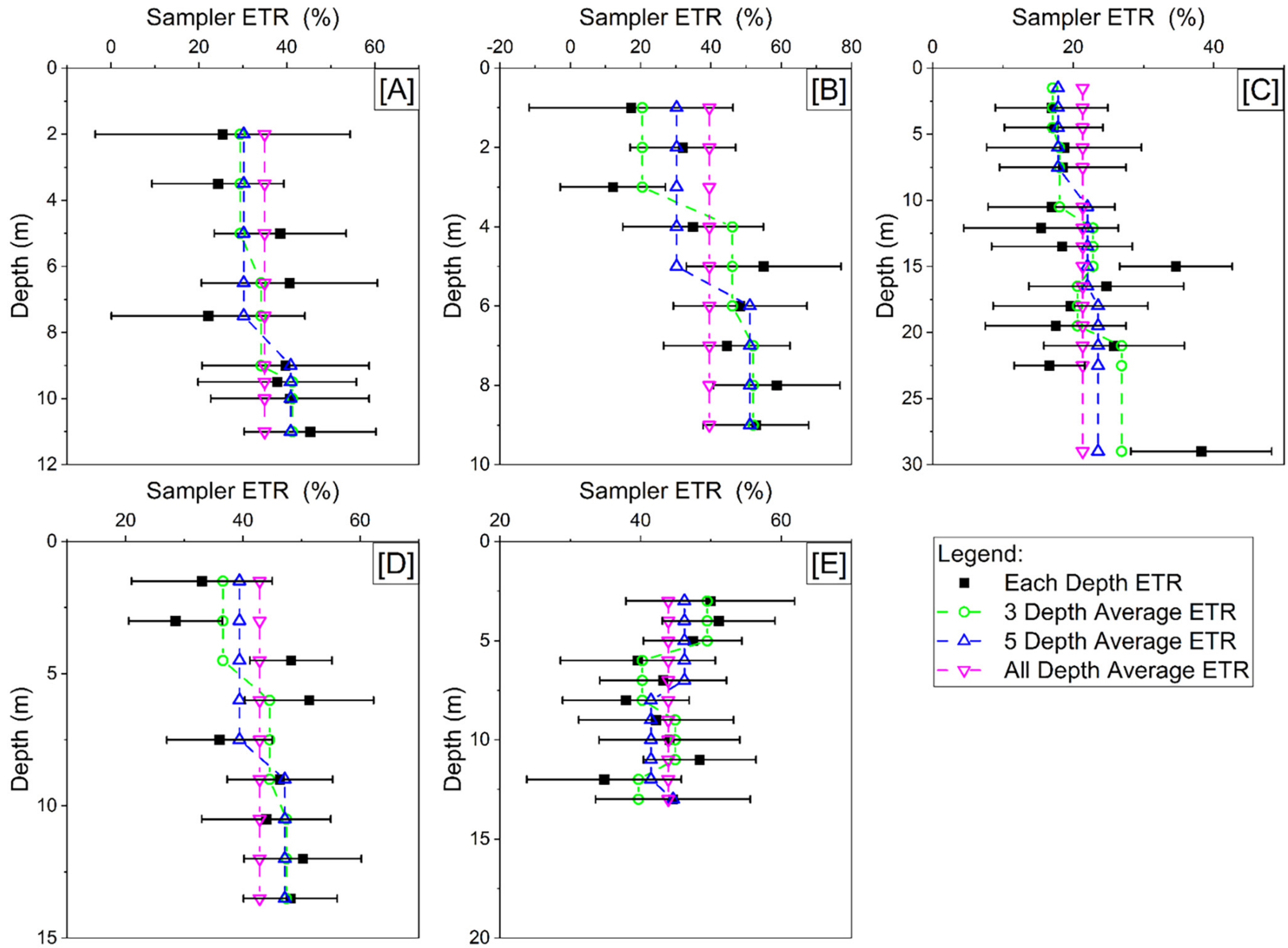

Fig. 13. Borehole-wise comparison of Sampler ETR (%) across different rigs: [A] RMH, [B] RSH, [C] HSH, [D] HTH, and [E] MAH; showing individual depth ETR values with error bars representing SD of blow-wise ETR measurements, along with 3-depth, 5-depth, and all-depth average ETR trend.

depths, N-value ranges, and soil types at five project sites (Sites A to E). Despite relatively uniform soil conditions at each site, the observed ETR values show substantial variability both within and across rigs, highlighting the limitations of using a single assumed ETR for SPT interpretation. For example, in Fig. 14, the HSH rig at Site A exhibits an anvil-level mean ETR ranging from approximately 28% to 77% depending on depth and N-value, with sampler-level ETRs ranging from 15% to over 45%. While the rig mean ETR (solid blue triangle) for HSH remains around 46% at the anvil and 20% at the sampler, individual tests frequently deviate by more than ±15%. Fig. 15 expands the comparison across three rigs (HTH, RMH, RSH) at Site A, where anvil-level ETRs for RMH approach 72%, whereas HTH and RSH stay close to 60%, highlighting equipment-specific transfer efficiencies. Similarly, sampler-level ETRs range from as low as 12% to over 55% across rigs. At Site B (Fig. 16), the MAH rig records consistently higher anvil ETRs (~75–90%) and sampler ETRs (~40–60%) compared to HSH and HTH rigs at the same site. This pattern persists at Sites C and D (Figs. 17 and 18), where the RMH rig maintains an anvil ETR above 60% for most cases, while sampler ETR fluctuates widely (20–50%). Even at the shallow depths of Site E (Fig. 19), ETR values span a wide range across rigs, despite similar soil types.

These differences are further reflected in the multiple horizontal markers (line-scatter plot): rig mean (blue triangle), site mean (magenta inverted triangle), N-value mean (red box), depth mean (green circle), and all-site mean (purple rhombus), which reveal how mean ETR trends are influenced by various parameters. For example, while the all-site mean anvil ETR remains around 60–65%, individual depth or N-value group means can diverge significantly by up to ±20%. This evidence clearly indicates that ETR is not only rig-dependent but also sensitive to depth and N-value. A comparative grouping of ETR with respect to depth, N-value ranges, and soil types (Figs. 14–19) indicates that depth and rig configuration exert a stronger influence on ETR variability than soil classification under the relatively uniform subsurface conditions at the study sites. If soil variability were higher, it could further increase the variability in both energy transfer and penetration resistance. Thus, the results indicate that energy measure-

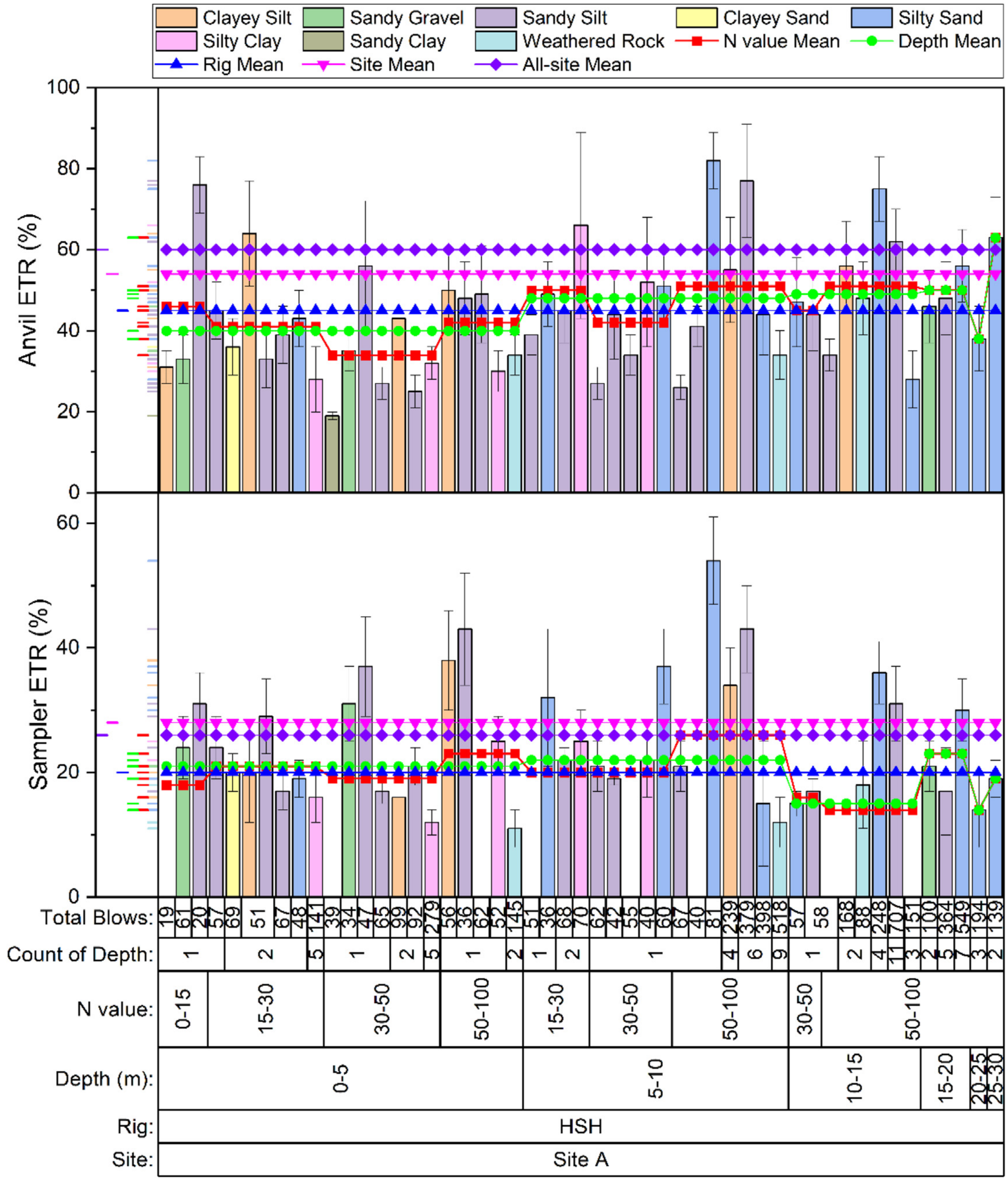

Fig. 14. Comparison of HSH rig anvil-level and sampler-level ETR (%) for different depths, N-value ranges, and soil types at Site A, with mean ETR trends shown for N-value, depth, rig, site, and all-site averages.

ment at representative depths, or where practical across every SPT test, is required to improve the reliability of N-value corrections, compared with relying solely on limited-depth measurements or average rig/site assumptions, which may mask substantial variability.

The observed ETR attenuation between the anvil and the sampler level generally ranges from ~15 to 25% and is consistent with values reported in previous studies. Earlier studies have indicated that ETR reductions due to rod length, couplings, and wave propagation effects range from 10 to 30%, depending on the SPT component configuration (Hong et al., 2022; Lukiantchuki et al., 2017; Odebrecht et al., 2005; Yadhunandan and Anbazhagan, 2026, 2025), and also due to the rod-dependant ETR estimation method (Eq. (1)) (Yadhunandan and Anbazhagan, 2026). Standard correction frameworks often incorporate rod-length correction factors to account for this form of energy dissipation. However, very few studies have directly measured energy at the sampler level under field conditions and the rod-length-independent method (FVCD method, Eq. (2). In most of the previous studies, energy losses are estimated indirectly using correction factors or theoretical

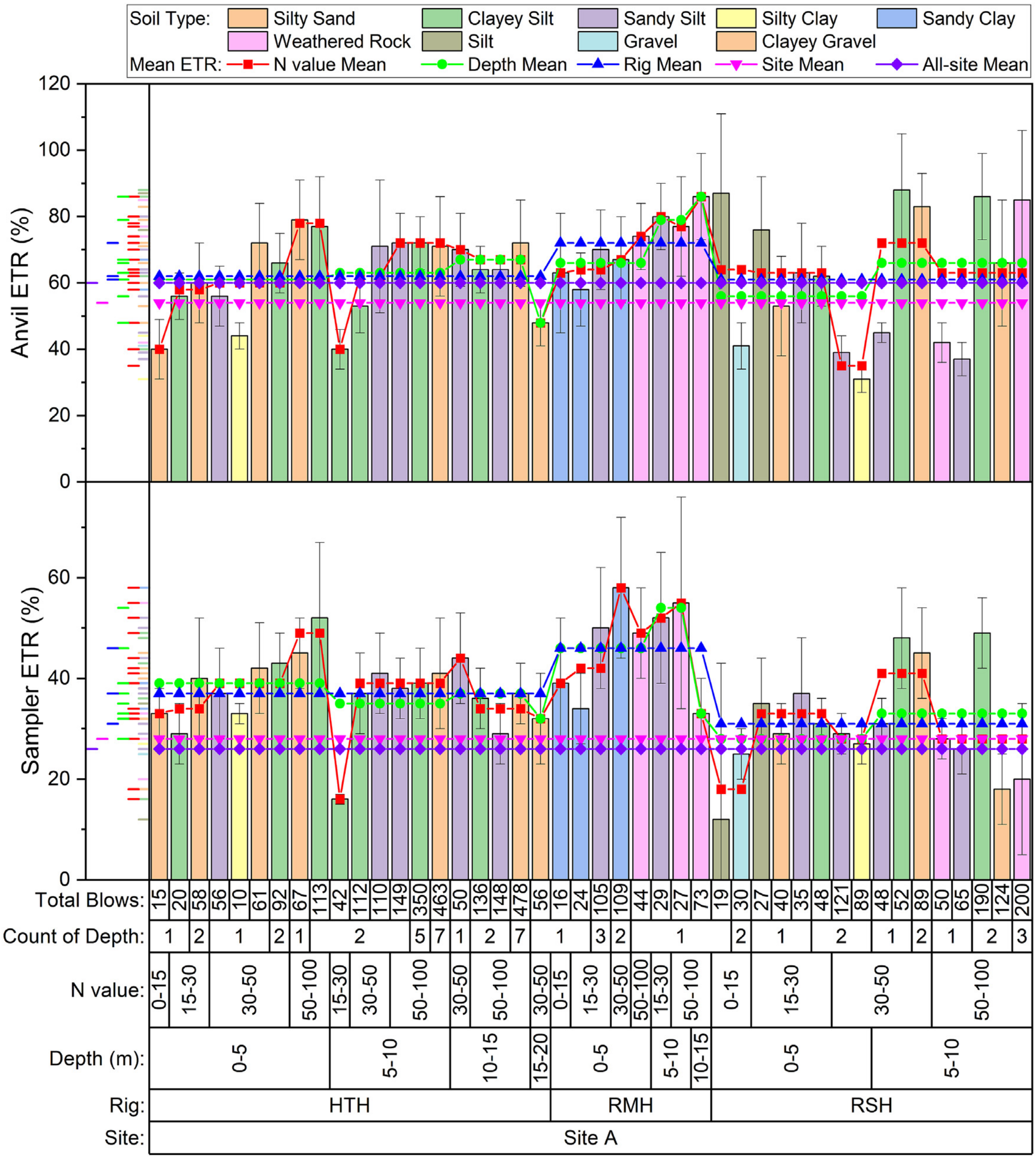

Fig. 15. Comparison of anvil-level and sampler-level ETR (%) for different rigs, depths, N-value ranges, and soil types at Site A, with mean ETR trends shown for N-value, depth, rig, site, and all-site averages.

approaches. In contrast, this study directly measures and quantifies energy attenuation from the anvil to the sampler across different rigs and depths and also uses a reliable ETR estimation approach based on the FVCD method (Eq. (2)). Furthermore, the rod lengths ranged from 0.5 to 30 m, with multiple joints and different hammer mechanisms, which reasonably explain the measured energy loss. At the same time, the results show that assuming negligible rod transmission loss can lead to errors in corrected N-values.

Furthermore, Fig. 20 presents a consolidated comparison of the ETR with SD error bars for various rigs tested across five geotechnical sites with relatively uniform soil conditions. The data are shown for both anvil-level (Fig. 20(a)) and sampler-level (Fig. 20(b)) instrumentation. For each rig, the number of blows, SPTs, and boreholes is annotated, providing important context on data density and coverage. At the anvil level, ETR values ranged from as low as 29 ± 5% (HSH_3 at Site A) to as high as 78 ± 15% (MAH_1 at Site B). Similarly, rigs such as RMH_1 and HSH_2 at Site A recorded high anvil ETRs of 74 ± 13% and 74 ± 17%, respectively, whereas rigs such as RSH_1 and RSH_2 reported much lower ETRs around 37%. Even within the same site and for the same rig type

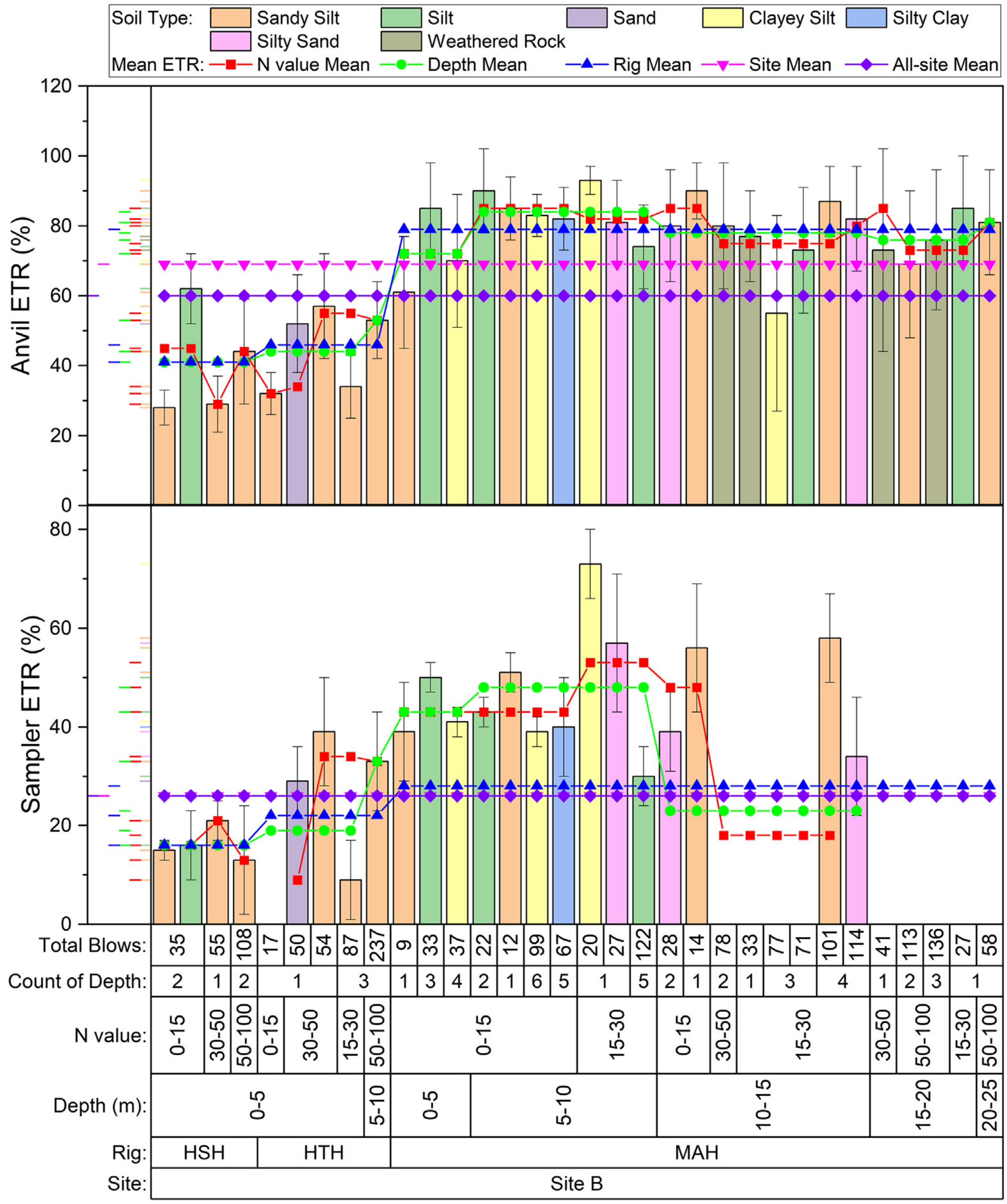

Fig. 16. Comparison of anvil-level and sampler-level ETR (%) for different rigs, depths, N-value ranges, and soil types at Site B, with mean ETR trends shown for N-value, depth, rig, site, and all-site averages.

(e.g., HSH series at Site A), the variation in ETR was substantial, highlighting the inconsistent performance under seemingly uniform conditions. At the sampler level, ETR values were even more variable and generally lower, ranging from 21% ± 3% (HSH_3 at Site A) to 54% ± 13% (RMH_1 at Site A). Many rigs recorded sampler ETRs in the range of 33–44%, with notable outliers at both ends. The difference between anvil and sampler ETRs for the same rig frequently exceeded 10–20%, confirming substantial energy losses down the drill rods.

These rig-wise comparisons reinforce a critical point that, even under the same project, site, and supervision, rigs can behave very differently in terms of energy transfer. Such discrepancies indicate that standardized or assumed rig efficiency values are inadequate, especially for projects involving multiple rigs or contractors. The findings support the adoption of more comprehensive, full-depth, test-specific energy measurements for every borehole to improve the reliability and accuracy of N-value corrections, particularly for critical and large-scale geotechnical investigations.

The observed ETR ranges in this study (approximately 29% to 90% at the anvil level and 10% to 60% at the sampler level) are generally consistent with the wide ranges reported in previous international investigations (Table A1; Aoki et al., 2007; Matsumoto et al., 2015; Sumanth et al., 2022). However, unlike many earlier studies that relied on limited-depth measurements or averaged

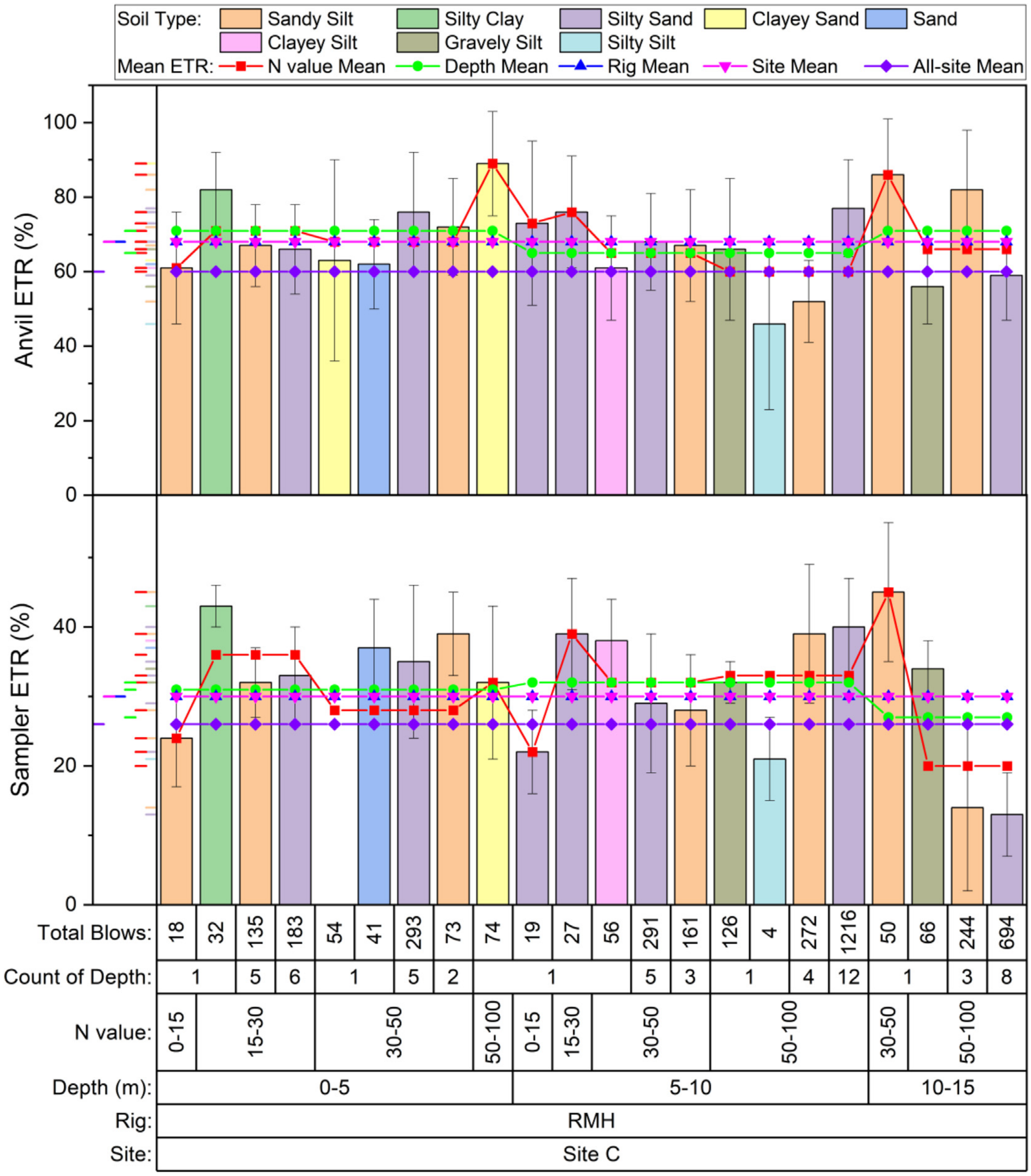

Fig. 17. Comparison of anvil-level and sampler-level ETR (%) for different rigs, depths, N-value ranges, and soil types at Site C, with mean ETR trends shown for N-value, depth, rig, site, and all-site averages.

rig efficiencies, the present study observed significant blow-wise and depth-wise variability within the same project site under uniform soil conditions. The results clearly show that even rigs of the same type can exhibit noticeably different energy-transfer behaviour. This reinforces the limitation of adopting a single representative ETR value for a rig, or borehole, or site, or project, and highlights the practical need for more comprehensive full-depth energy monitoring.

4. Conclusions

This study comprehensively evaluated hammer energy transfer during SPT, comparing a commercial 4-channel system with a custom-developed 2-channel system designed to measure energy at both the anvil and sampler levels. The study presented the results of 42 laboratory SPT tests and 314 field SPT tests, totaling over 20,000 hammer blows, at sites with uniform soil layers and conditions to isolate the effects of equipment variability on the ETR.

The study successfully evaluated and compared the custom 2-channel system with 5000g or 10,000g accelerometers against a commercial 4-channel system with 10,000g accelerometers. Results from both laboratory (42 SPTs, 821 blows) and field (314 SPTs, 20,448 blows) tests showed good agreement, with ETR differences typically within ±5%. This indicates that a 2-channel system with a 5000g accelerometer is sufficient to capture SPT dynamics, mak-

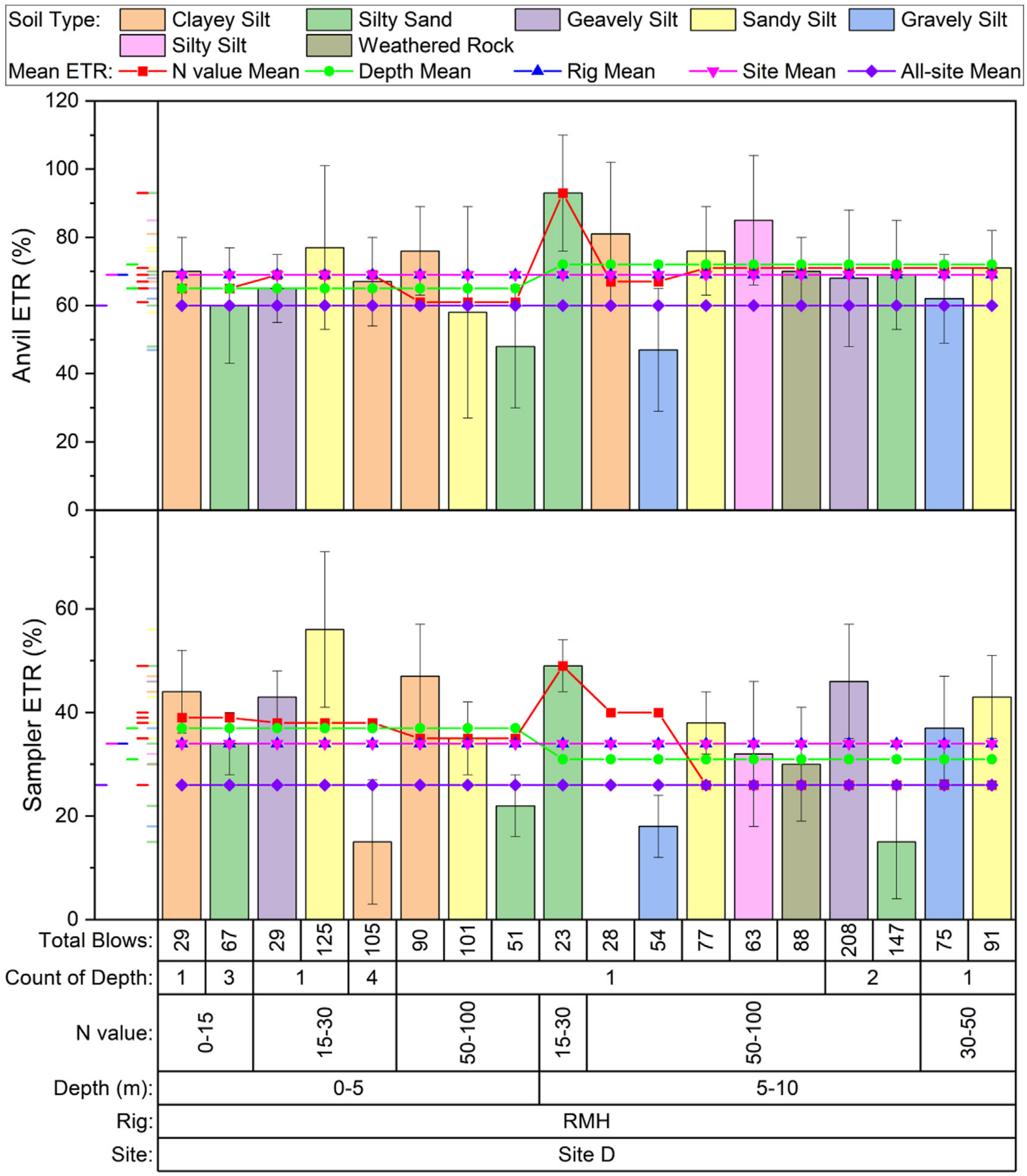

Fig. 18. Comparison of anvil-level and sampler-level ETR (%) for different rigs, depths, N-value ranges, and soil types at Site D, with mean ETR trends shown for N-value, depth, rig, site, and all-site averages.

ing it a more economical and practical option for testing. In general, either a 2-channel or 4-channel system, with 5000g or 10,000g accelerometers, is adequate for SPT energy measurements and can be selected based on practical feasibility. A key advantage of the custom 2-channel system is that it enables easy, convenient measurement of energy at the sampler level, providing a more direct assessment of energy transfer to the soil.

The study also demonstrated significant ETR variability across different rigs operating at the same site under identical soil layers and conditions. Anvil ETRs ranged from as low as 29% to as high as 78%. Similarly, sampler ETRs ranged from 21% to 54%. The results show that energy transfer is strongly influenced by rig type and hammer mechanism, with automatic systems generally exhibiting more consistent performance compared to manual or semi-mechanical systems. In addition, ETR exhibited depth-dependent trends, which may be attributed to increasing rod length, cumulative joint effects, and wave attenuation along the drill string. Variations across soil types and N-value ranges further indicate that changes in penetration resistance alter stress-wave transmission characteristics, thereby affecting the measured energy transfer. This highlights that energy transfer is not only dependent on the rig but is also highly sensitive to testing depth and N-value. These findings suggest that ETR is governed by

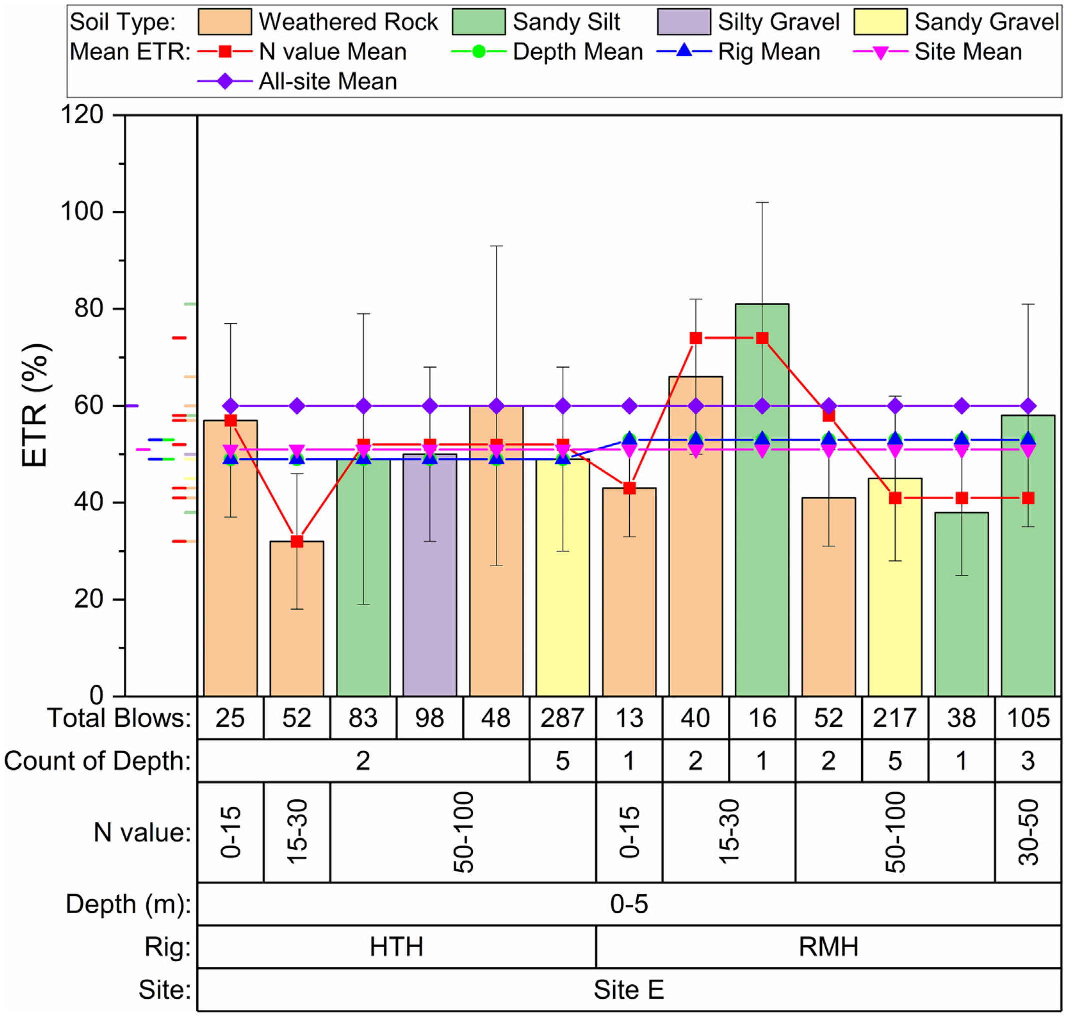

Fig. 19. Comparison of anvil-level ETR (%) for different rigs, depths, N-value ranges, and soil types at Site E (sampler-level data were not available at this site), with mean ETR trends shown for N-value, depth, rig, site, and all-site averages.

a combined influence of equipment configuration, rod system characteristics, and soil resistance conditions. Therefore, the results suggest that using assumed or average ETR values from 3 or 5 depth recordings, as permitted in some current practice, may completely mask substantial variability and may lead to inaccurate N-value corrections and misleading geotechnical interpretations.

In current geotechnical design practice and codes, typical ETR values are taken for different hammer types, and rod-length corrections are often applied using generalized factors. However, the present study found that energy transfer and its losses between the anvil and sampler levels are not constant and can vary significantly with rig configuration, rod length, depth, and soil type. By directly measuring anvil and sampler-level energy for all the SPT tests, this research provides quantitative insight into actual rod transmission losses. These findings contribute to geotechnical practice by supporting more reliable SPT N normalization, particularly in projects involving multiple rigs or critical infrastructure.

CRediT authorship contribution statement

M.E. Yadhunandan: Writing – original draft, Visualization, Validation, Software, Methodology, Investigation, Data curation, Conceptualization. **P. Anbazhagan:** Writing – review & editing, Visualization, Validation, Supervision, Resources, Funding acquisition, Conceptualization.

Funding

This work was supported by the SERB, DST, Govt. of India for the project “Development of correction factors for standard penetration test N values in India through energy measurement and field experiments – Step towards a reliable Liquefaction Potential Assessment” under Grant SERB/F/198/2017-18 dated 11/05/2017; and Dam Safety (Rehabilitation) Directorate, Central Water Commission (CWC) for funding the “International Centre of Excellence in Dam Engineering” (ICoEDE) under the Dam Rehabilitation and Improvement Project (DRIP); Ministry of Jal

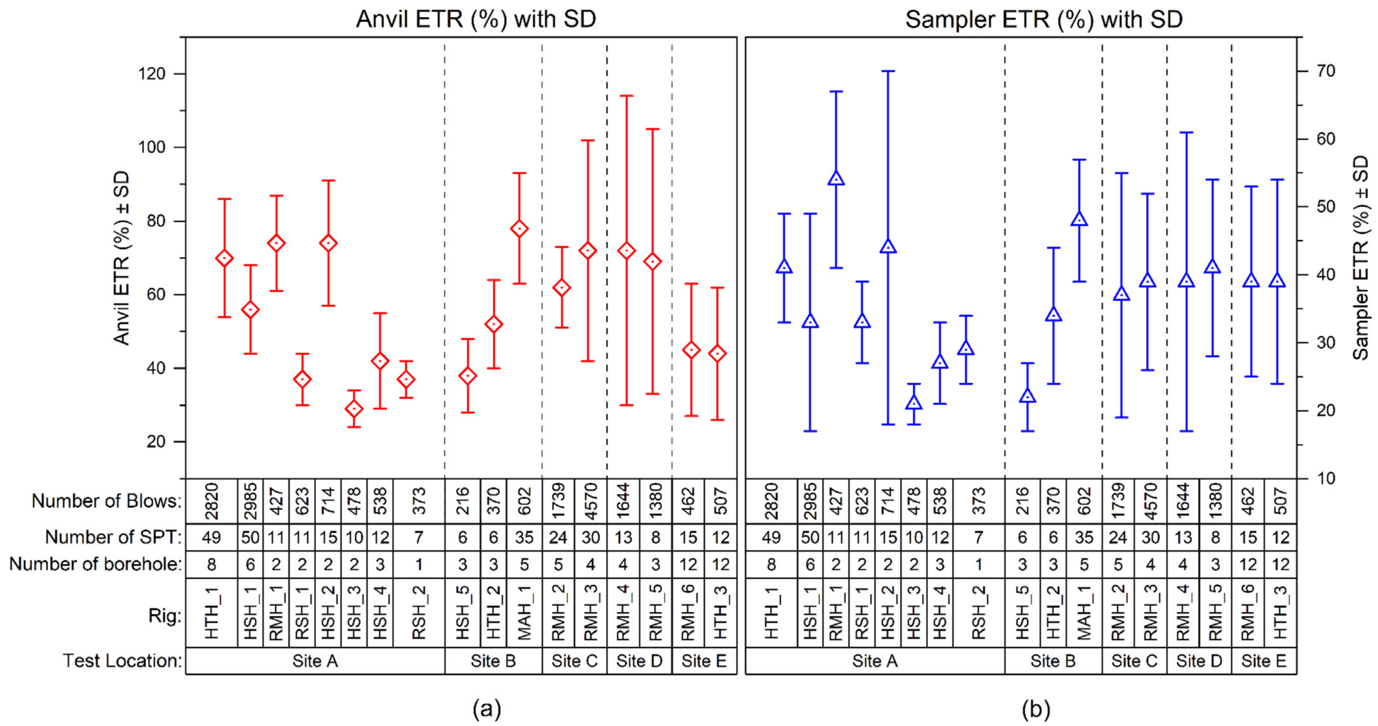

Fig. 20. Comparison of ETR with SD error bars at (a) the Anvil and (b) the Sampler level for different rigs at the same site with relatively uniform soil conditions.

Shakti (MoJS), Government of India for the project entitled "Integrated Investigation for Risk Assessment of the Dam" under grant R-24011/57/2023-Pen Riv Section-MOWR.

Acknowledgement

The authors thank Mr. Selvam, Mr. Athiyaman, Mr. Kannan, and Mr. Katta Govindu, Somehsa Geo-Coastal Pvt Ltd (SMG), Bangalore, for their valuable support during field and laboratory SPT tests using the SPT Analyzer. The authors also thank Mr. Sanni Babu, M.Tech student; Mr. Rahul and Mr. Suhas, internship students; Dr. Ayush Kumar, Research Assistant, Department of Civil Engineering, Indian Institute of Science, for their valuable assistance during field SPT testing and other support related to this work.

All research described in this paper was conducted in accordance with institutional ethical guidelines. All necessary permits and approvals for conducting field and observational work at the study sites were secured from the relevant authorities prior to the commencement of the research.

Data availability

Data generated or analyzed during this study are available from the corresponding author upon reasonable request.

Appendix A.

Table A1

Review of instrumentation and field configurations in SPT ETR studies (Ns – Not specified).

SN	Author(s) & Year	Year	ETR (%)	Load Cell Capacity	Accelremeter Capacity (g)	Rig Type	Hammer Type	Rod Type	Study/Focus
1	Kovacs et al. (1977)	1977	25-70% (cathead & rope)	Ns	Ns	Truck-mounted rig with Safe-T-Driver	63.5 kg enclosed sleeve-type hammer	Standard SPT AW rods	Hammer lifting comparison for energy consistency.
2	Schmertmann and Palacios (1979)	1979	30-80%, typically ~50%	Dynamic load cell, ~40,000 lb capacity; calibration ±1%	Ns	Florida DOT drill rigs (11 rigs tested)	63.5 kg (140 lb) rope & cathead	Standard SPT AW rods	Rod/hammer energy effect modeled via wave theory.
3	Kovacs and Salomone (1982)	1982	30–98%	Ns	Ns	Field rigs with instrumented split spoon	Donut, Safety, Automatic, Rope-pulled	SPT rods (Ns)	ETR measured by force and velocity methods.
4	Tokimatsu and Yoshimi (1983)	1983	Ns	Ns	Ns	Japanese geotechnical rigs	Donut hammer, rope and cathead	Standard SPT AW rods	SPT practices vary across Japan; ETR varies.
5	Riggs et al. (1984)	1984	Auto hammer: ~89%, Cathead: ~70-100%	Binary Instruments Model 102 SPY Calibrator	Ns	CME-450, CME-55, CME-45B, CME-75	CME 140-lb Automatic vs. Cathead & rope (safety hammer)	5-ft AW parallel wall drill rods	Auto hammers more consistent in ETR delivery.
6	Sy and Campanella (1991)	1991	Measured Energy; exact value not reported, compared to theoretical	Ns	Ns	Field tests; rigs not detailed	Ns; consistent with ASTM D1586 setups	Steel rods; correction for wave speed and length used	Proposed FV method to avoid cutoff errors.
7	Decourt and Quaresma (1994)	1994	~72% for Brazilian SPT	Not applicable	Not applicable	Brazilian rigs with SPT-T torque setup	63.5 kg manual rope hammer	Standard SPT AW rods	SPT-T method for torque-based validation.
8	Clayton (1995)	1995	45-90%	Ns	Ns	Various UK rigs	Donut, trip release, automatic	Standard SPT AW rods	Theoretical framework for ETR measurement.

(*continued on next page*)

Table A1 (*continued*)

SN	Author(s) & Year	Year	ETR (%)	Load Cell Capacity	Accelremeter Capacity (g)	Rig Type	Hammer Type	Rod Type	Study/Focus
9	Abou-matar and Goble (1997)	1997	35-75%	Ns	Ns	Laboratory drop setup (CME safety hammer system)	Safety hammer (CME), drop height 760 mm	AW rod (6 m total), connected via commercial connectors	GRLWEAP-based lab tests; force vs velocity error.
10	Zhang (1999)	1999	Ns	Not used; literature-based analysis	Ns	Generic assumed	Referenced ASTM-standard SPT	Standard SPT AW rods	Used N-value, no ETR testing performed.
11	Aggour and Radding (2001)	2001	45-70%	Ns	Ns	Field SPT with various rigs (manual and automatic hammers considered)	63.5 kg hammer (manual and automatic variations)	Standard SPT AW rods	Manual vs auto hammer ER reviewed.
12	Youd and Idriss (2001)	2001	Ns	Not measured	Ns	General US rigs	Referenced manual and automatic	Standard SPT AW rods	Guidelines on energy standardization for liquefaction.
13	Lim et al. (2002)	2002	Ns	Not applicable	Not applicable	Pile driving with 7000 kg hammer	7000 kg drop hammer	Pile-type rods (not SPT)	HSC tracked pile rebound visually.
14	Daniel et al. (2003)	2003	Ns	DEM system by BC Hydro	5000/10000 (referenced)	Truck-mounted + others	Donut, Safety, Trip-release	SPT rods, LPT rods	LPT vs SPT energy compared and corrected.
15	Odebrecht et al. (2005)	2005	32-87%	Ns	Ns	Manual + automatic release (Brazilian rigs)	Donut, Trip, Auto	Standard SPT AW rods	Thesis covering SPT energy configurations.
16	Daniel et al. (2005)	2005	Ns	Ns	5000/10000 (referenced)	Field tests; rigs not detailed	Donut	Short vs. standard rods	Short rod system energy corrections studied.
17	Rogers (2006)	2006	Manual: 45%, Safety: ~60%, Auto: 80-90%	Ns	Ns	General teaching reference	Donut, Safety, Automatic	Standard SPT AW rods	Historical ETR corrections reviewed.
18	Rodrigues et al. (2008)	2008	Ns	Ns	Ns	Pagani TG 73-200	63.5 kg drop hammer	Massive vs. Hollow (1 m, ~6.3 kg/m)	400 blows: rod type had minor ETR effect.

Table A1 (*continued*)

SN	Author(s) & Year	Year	ETR (%)	Load Cell Capacity	Accelremeter Capacity (g)	Rig Type	Hammer Type	Rod Type	Study/Focus
19	Youd et al. (2008)	2008	40-90%	Ns	Ns	Field SPT rigs (USA)	SPT donut hammer (various drop heights)	Standard SPT AW rods	Drop height influence on ETR studied.
20	Lee et al. (2010)	2010	Varies with N-value, Up to +3.2% increase due to type-I secondary impact	600 mm instrumented rod with PDA	Ns	Rotary wash boring machine	Donut and Modified Automatic Donut (MAD)	Standard SPT AW rods	Type-I impacts increase ETR; Type-II don't.
21	Dung et al. (2011)	2011	90%	Ns	Ns	Rotary wash boring machine	Donut hammer, manual cathead (2.25 rope turns)	Type A (41.3 mm OD, 5.7 kg/m)	PDA used for toe resistance validation.
22	Yimsiri (2013)	2013	Donut: 49%, Safety: 68%, Trip: 95%	350 Î© strain gauge (calibrated for 100 kN)	10,000	SPT rigs (Thailand)	Donut, Safety, Trip	AW rods (830 mm instrumented)	Thai SPT benchmarked via FV/F^2 methods.
23	Lee et al. (2014)	2014	~74.32%	Ns; PDA used	Ns	Rotary wash boring machine	Donut (manual rope-pulley)	AW rods, 600 mm instrumented	Line-scan camera shows impact types.
24	Matsumoto et al. (2015)	2015	Manual: ~45-60%, Automatic: ~60-70%)	Ns	Ns	Conventional SPT rigs in Japan	Manual trip & automatic trip	Standard AW/NW	SPT and DCPT energy compared.
25	Look (2016)	2016	Varies; digital vs manual shows 20% error; PDM vs PDA showed different energy values	PDA: Load + Accel sensors; PDM: Infrared laser tracker	Ns	Ns; field rigs in Australia	Automatic trip hammer	Standard rods; placement below anvil and above sampler	PDA vs PDM showed blow energy variations.
26	Batilas et al. (2017)	2017	Manual: 46±3.8%, Automatic: 77±4.6%	Ns	Ns	Various rigs in Greece	Donut hammer, manual vs automatic release	Standard rods, donut hammer setup	900+ field recordings; release type impacts ETR.
27	Moghaddam et al. (2017)	2017	Varies, ER normalized to 70%	Not detailed	Ns	Various Texas rigs (TxDOT studies)	Auto-trip and cathead (TxDOT rigs)	Standard TxDOT rods	SPT design updated with ETR corrections.

(*continued on next page*)

Table A1 (*continued*)

SN	Author(s) & Year	Year	ETR (%)	Load Cell Capacity	Accelremeter Capacity (g)	Rig Type	Hammer Type	Rod Type	Study/Focus
28	Ghafghazi (2017)	2017	SPT normalized to N_{60} (60%)	Integrated iBPT sensors (force and acceleration)	Not in g, but % of ICE 180 hammer energy (10.85 kJ)	iBPT and SPT at 4 different dam sites (USA)	ICE 180 diesel hammer (iBPT); Standard 63.5 kg SPT hammer	Standard Becker & SPT rods	iBPT vs SPT N-value relation made.
29	Lukiantchuki et al. (2017)	2017	Top: ~65%, Bottom: ~50-60%	Strain gauge, accelerometer (top and near sampler)	5000	Brazilian rigs	Hand-lifted & auto-trip	Instrumented rods above sampler and below anvil	Manual hammers: energy dispersion noted.
30	Anbazhagan et al. (2021)	2021	Used: 60% (corrections from 25-85% possible)	Ns	Ns	Field tests; rigs not detailed	Varies by region (assumes donut/safety hammer)	Ns	Gmax correlations with varying ETR.
31	Anbazhagan et al. (2022b)	2022	Varies; 25-95% observed	240 kN	10,000	Rotary and Hydraulic rigs	Donut (Manual and Cathead release)	Standard SPT AW rods	SBC and depth effects due to ETR.
32	Anbazhagan et al. (2022a)	2022	Varies; used energy-based correction (ETR)	240 kN	10,000	Rotary and Hydraulic rigs	Donut (Manual and Cathead release)	Standard SPT AW rods	HEMA vs Analyzer system (2-ch vs 4-ch).
33	Hong et al. (2022)	2022	Ns	617.04 kN	100,000g	Rotary wash boring rig	Automatic trip hammer	Standard SPT AW rods	Strain-based e-module tracked sampler energy.
34	Sumanth et al. (2022)	2022	20-90%, depending on rig-hammer combo	Ns	Ns	Calyx, TRD-300, multipurpose rigs	Donut (rope/ hydraulic), auto-trip, automatic	Standard SPT AW rods	India-wide rig dataset analyzed for ETR.
35	Morgano and Liang (2022)	2022	Energy reduction up to 20% for short rods	Ns	Ns	Field tests; rigs not detailed	Donut	Standard SPT AW rods	Rod length vs energy loss analyzed.
36	Tan and Ramli (2023)	2023	60% (normalized)	Ns	Ns	Field tests; rigs not detailed	Various	Varies (length correction)	Energy correction effects on Su estimation.

References

Abou-matar, H., Goble, G.G., 1997. SPT dynamic analysis and measurements. J. Geotech. Geoenviron. Eng. 123, 921–928. https://doi.org/10.1061/(ASCE)1090-0241(1997)123:10(921).

Aggour, M.S., Radding, W.R., 2001. Standard penetration test (SPT) correction (Technical Research Report No. MD-02-007B48). University of Maryland, Maryland. DOI: onlinepubs.trb.org/onlinepubs/trispdfs/00929164.pdf.

Anbazhagan, P., Ayush, K., Yadhunandan, M.E., Siriwanth, K., Suryanarayana, K., Sahodar, G., 2022a. Effective use of SPT: hammer energy measurement and integrated subsurface investigation. Indian Geotech J 52, 1079–1096. https://doi.org/10.1007/s40098-022-00609-z.

Anbazhagan, P., Kumar, A., Ingale, S.G., Jha, S.K., Lenin, K.R., 2021. Shear modulus from SPT N-values with different energy values. Soil Dyn. Earthq. Eng. 150. https://doi.org/10.1016/j.soildyn.2021.106925 106925.

Anbazhagan, P., Yadhunandan, M.E., Kumar, A., 2022b. Effects of hammer energy on borehole termination and SBC calculation through site-specific hammer energy measurement using SPT HEMA. Indian Geotech J 52, 381–399. https://doi.org/10.1007/s40098-021-00582-z.

Aoki, N., Esquivel, E.R., Neves, L.F.S., Cintra, J.C.A., 2007. The impact efficiency obtained from static load test performed on the SPT sampler. Soils Found. 47, 1045–1052. https://doi.org/10.3208/sandf.47.1045.

AS 1289.6.3.1, 2004. Australian Standard, ‘‘Methods of testing soils for engineering purposes, soil strength and consolidation tests, determination of the penetration resistance of a soil Standard penetration test (SPT).

ASTM Standard D1586-18 - Standard Test Method for Standard Penetration Test (SPT) and Split-Barrel Sampling of Soils, 2018. DOI: 10.1520/D1586_D1586M-18E01.

ASTM Standard D4633-16 - Standard Test Method for Energy Measurement for Dynamic Penetrometers, 2016. https://doi.org/10.1520/D4633-16.

ASTM Standard D6066-11, 2011. Standard practice for determining the normalized penetration resistance of sands for evaluation of liquefaction potential. https://doi.org/10.1520/d6066-11.

Batilas, A.V., Pelekis, P.C., Roussos, P.G., Athanasopoulos, G.A., 2017. SPT energy measurements: manual vs. automatic hammer release. Geotech. Geol. Eng. 35, 879–888. https://doi.org/10.1007/s10706-016-0138-z.

BIS 1893 (Part 1): 2016 - Criteria for Earthquake Resistant Design of Structures, 2016.

Bolton Seed, H., Tokimatsu, K., Harder, L.F., Chung, R.M., 1985. Influence of SPT procedures in soil liquefaction resistance evaluations. J. Geotech. Eng. 111, 1425–1445. https://doi.org/10.1061/(ASCE)0733-9410(1985)111:12(1425).

Briaud, J.-L., Gibbens, R., 1999. Behavior of five large spread footings in sand. J. Geotech. Geoenviron. Eng. 125, 787–796. https://doi.org/10.1061/(ASCE)1090-0241(1999)125:9(787).

BS EN ISO 22476-3:2005+A1:2011 - Geotechnical investigation and testing — Field testing — Part 3: Standard penetration test, 2005.

Clayton, C.R., 1995. The standard penetration test (SPT): methods and use. Ciria.

Cubrinovski, M., Ishihara, K., 1999. Empirical correlation between SPT N-value and relative density for sandy soils. Soils Found. 39, 61–71. https://doi.org/10.3208/sandf.39.5_61.

Daniel, C.R., Howie, J.A., 2005. Effect of Hammer Shape On Energy Transfer Measurement in the Standard Penetration Test11) By Jiin - Song Tsai, Yean-Jhe Liou, Fu-Chen Liu and Chin-Huei Chen, Vol. 44, No. 3, June 2004, pp. 103–114. Soils Found. 45, 121–126. https://doi.org/10.3208/sandf.45.5_121.

Daniel, C.R., Howie, J.A., Jackson, R.S., Walker, B., 2005. Review of standard penetration test short rod corrections. J. Geotech. Geoenviron. Eng. 131, 489–497. https://doi.org/10.1061/(ASCE)1090-0241(2005)131:4(489).

Daniel, C.R., Howie, J.A., Sy, A., 2003. A method for correlating large penetration test (LPT) to standard penetration test (SPT) blow counts. Can. Geotech. J. 40, 66–77. https://doi.org/10.1139/t02-094.

Decourt, L., Quaresma, A.R., 1994. Practical applications of the standard penetration test complemented by torque measurements, SPT-T; present stage and future trends. Presented at the 13th International conference on soil mechanics and foundation engineering, New Delhi, pp. 143–146.

Dung, N.T., Chung, S.G., Kim, S.R., Beak, S.H., 2011. Applicability of the SPT-based methods for estimating toe bearing capacity of driven PHC piles in the thick deltaic deposits. KSCE J. Civ. Eng. 15, 1023–1031. https://doi.org/10.1007/s12205-011-0801-0.

GB 50021-2001 Code for investigation of geotechnical engineering, GB 50021-2001 (2009 modified edition), 2001.

Ghafghazi, M., DeJong, J.T., Sturm, A.P., Temple, C.E., 2017. Instrumented Becker penetration test. II: iBPT-SPT correlation for characterization and liquefaction assessment of gravelly soils. J. Geotech. Geoenviron. Eng. 143. https://doi.org/10.1061/(ASCE)GT.1943-5606.0001718 04017063.

Guan, Z., Wang, Y., 2020. Selection of standard penetration test number for geotechnical investigation of a vertical cross section considering spatial variability and correlation in soil properties. Can. Geotech. J. 58, 1654–1668. https://doi.org/10.1139/cgj-2020-0440.

Honeycutt, J.N., Kiser, S.E., Anderson, J.B., 2014. Database evaluation of energy transfer for central mine equipment automatic hammer standard penetration tests. J. Geotech. Geoenviron. Eng. 140, 194–200. https://doi.org/10.1061/(ASCE)GT.1943-5606.0000988.

Hong, W.-T., Kim, S.Y., Lee, J.-S., 2022. Evaluation of driving energy transferred to split spoon sampler for accuracy improvement of standard penetration test. Measurement 188. https://doi.org/10.1016/j.measurement.2021.110384 110384.

Howie, J.A., Daniel, C.R., Jackson, R.S., Walker, B., Sy, A., 2003. Comparison of energy measurement methods in the standard penetration test: final report, appendices I, II, III, and IV (Technical Research Report). University of British Columbia. Geotechnical Research Group.

JIS 1219, 2013. Japanese standards association. Method for Standard Penetration Test.

Juang, C., Fang, S., Tang, W., Khor, E., Kung, G.-T.-C., Zhang, J., 2009. Evaluating model uncertainty of an SPT-based Simplified method for reliability analysis for probability of liquefaction. Soils Found. 49, 135–152. https://doi.org/10.3208/sandf.49.135.

Kovacs, W.D., Evans, J.C., Griffith, A.H., 1977. Towards a more standardized SPT. Proceedings of the Ninth International Conference on Soil Mechanics and Foundation Grain, pp. 269–276.

Kovacs, W.D., Salomone, L.A., 1982. SPT hammer energy measurement. J. Geotech. Eng. Div. 108, 599–620. https://doi.org/10.1061/AJGEB6.0001278.

Lee, C., An, S., Lee, W., 2014. Real-time monitoring of SPT donut hammer motion and SPT energy transfer ratio using digital line-scan camera and pile driving analyzer. Acta Geotech. 9, 959–968. https://doi.org/10.1007/s11440-012-0197-0.

Lee, C., Lee, J.-S., An, S., Lee, W., 2010. Effect of secondary impacts on SPT rod energy and sampler penetration. J. Geotech. Geoenviron. Eng. 136, 522–526. https://doi.org/10.1061/(ASCE)GT.1943-5606.0000236.

Lim, M.-S., You, B.-J., Oh, S.-R., Han, S.-S., Lee, S.-H., 2002. Visual precise measurement of pile rebound and penetration movement using a high-speed line-scan camera. Trans. Control Autom. Syst. Eng. 4, 341–346.

Look, B., 2016. The SPT N-value errors examined with digital technology. 5th International Society for Soil Mechanics, pp. 333–338.

Lukiantchuki, J.A., Bernardes, G.D.P., Esquivel, E.R., 2017. Energy Ratio (ER) for the standard penetration test based on measured field tests. SR 40, 77–91. https://doi.org/10.28927/SR.402077.

Matsumoto, T., Phan, L.T., Oshima, A., Shimono, S., 2015. Measurements of driving energy in SPT and various dynamic cone penetration tests. Soils Found. 55, 201–212. https://doi.org/10.1016/j.sandf.2014.12.016.

Moghaddam, R.B., Lawson, W.D., Surles, J.G., Seo, H., Jayawickrama, P.W., 2017. Hammer efficiency and correction factors for the TxDOT texas cone penetration test. Geotech. Geol. Eng. 35, 2147–2162. https://doi.org/10.1007/s10706-017-0234-8.

Morgano, C.M., Liang, R., 2022. Energy transfer in SPT–rod length effect. Application of Stress-Wave Theory to Piles. Routledge, pp. 121–127. https://doi.org/10.1201/9781315137544-26.

Muduli, P.K., Das, S.K., 2015. Model uncertainty of SPT-based method for evaluation of seismic soil liquefaction potential using multi-gene genetic programming. Soils Found. 55, 258–275. https://doi.org/10.1016/j.sandf.2015.02.003.

Odebrecht, E., Schnaid, F., Rocha, M.M., De Paula Bernardes, G., 2005. Energy efficiency for standard penetration tests. J. Geotech. Geoenviron. Eng. 131, 1252–1263. https://doi.org/10.1061/(ASCE)1090-0241(2005)131:10(1252).

Riggs, C., Mathes, G., Rassieur, C., 1984. A field study of an automatic SPT hammer system. Geotech. Test. J. 7, 158–163. https://doi.org/10.1520/GTJ10492J.

Rodrigues, C., Cavalcante, E.H., Danziger, B.R., Viana da Fonseca, A., 2008. Influence of rod type in SPT efficiency. Proceedings of the 8th International Conference on the Application of Stress Wave Theory Piles: Science, Technology and Practice. Jaime Alberto Santos, IST, pp. 731–736.

Rogers, J.D., 2006. Subsurface exploration using the standard penetration test and the cone penetrometer test. Environ. Eng. Geosci. 12, 161–179.

Schmertmann, J.H., Palacios, A., 1979. Energy dynamics of SPT. J. Geotech. Eng. Div. 105, 909–926. https://doi.org/10.1061/AJGEB6.0000839.

Skempton, A.W., 1986. Standard penetration test procedures and the effects in sands of overburden pressure, relative density, particle size, ageing and overconsolidation. Géotechnique 36, 425–447. https://doi.org/10.1680/geot.1986.36.3.425.

Sumanth, H.C., Parthasarathy, C.R., Nandhagopal, A.R., Ramachandra, A.S., 2022. Significance of energy transfer ratio in standard penetration test and its influence on foundation design. Indian Geotechnical Conference. Springer, pp. 269–282. https://doi.org/10.1007/978-981-97-1737-8_23.

Sy, A., Campanella, R.G., 1991. An alternate method of measuring SPT energy. Presented at the International Conferences on Recent Advances in Geotechnical Earthquake Engineering and Soil Dynamics.

Tan, J.J., Ramli, H., 2023. Effect of standard penetration test corrections on the estimation of undrained shear strength. J. Civ. Eng. Manag. 29, 501–515. https://doi.org/10.3846/jcem.2023.18441.

Tokimatsu, K., Yoshimi, Y., 1983. Empirical correlation of soil liquefaction based on SPT N-value and fines content. Soils Found. 23, 56–74. https://doi.org/10.3208/sandf1972.23.4_56.

Tsai, J.-S., Liou, Y.-J., Liu, F.-C., Chen, C.-H., 2004. Effect of hammer shape on energy transfer measurement in the standard penetration test. Soils Found. 44, 103–114. https://doi.org/10.3208/sandf.44.3_103.

Yadhunandan, M.E., Anbazhagan, P., 2026. A novel approach to reliable SPT hammer energy measurement using FVCD method with dual-instrumentation and visual measurement validation. Measurement 257 (Part A). https://doi.org/10.1016/j.measurement.2025.118498.

Yadhunandan, M.E., Anbazhagan, P., 2025. Effective visual measurement system for SPT hammer energy measurement. Measurement 253 (Part D). https://doi.org/10.1016/j.measurement.2025.117777.

Yimsiri, S., 2013. Energy ratio of SPT practice performed in Thailand. Geotechnical and Geophysical Site Characterization Presented at the 4th International Conference on Site Characterization (ISC-4). https://doi.org/10.1201/b15551-46.

Youd, T.L., Bartholomew, H.W., Steidl, J.H., 2008. SPT hammer energy ratio versus drop height. J. Geotech. Geoenviron. Eng. 134, 397–400. https://doi.org/10.1061/(ASCE)1090-0241(2008)134:3(397).

Youd, T.L., Idriss, I.M., 2001. Liquefaction resistance of soils: summary report from the 1996 NCEER and 1998 NCEER/NSF workshops on evaluation of liquefaction resistance of soils. J. Geotech. Geoenviron. Eng. 127, 297–313. https://doi.org/10.1061/(ASCE)1090-0241(2001)127:4(297).

Zhang, Z., 1999. Flexible camera calibration by viewing a plane from unknown orientations. In: Proceedings of the Seventh IEEE International Conference on Computer Vision, vol. 1, pp. 666–673. https://doi.org/10.1109/ICCV.1999.791289.